gear TECHNOLOGY®

JUNE 2025

Metrology
Off-Highway
Workholding

TECHNICAL

Nanocomposite Coatings for Gears

3D Scan-Based Reverse Engineering of Differential Bevel Gears

geartechnology.com

Gear Technology is POWERED by The American Gear Manufacturers Association

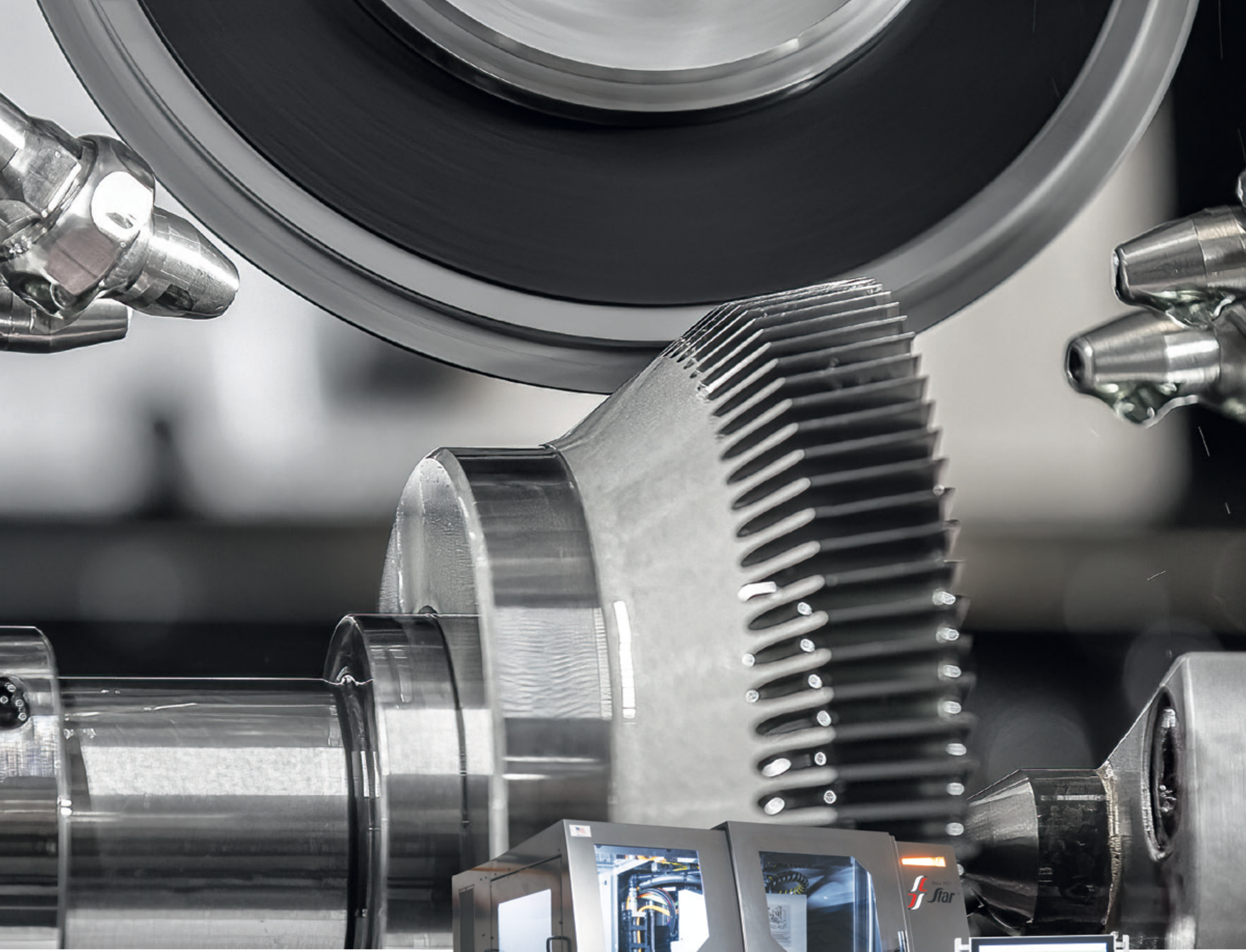


NXT

CONTENTS

gear TECHNOLOGY®

JUNE 2025

feature

16

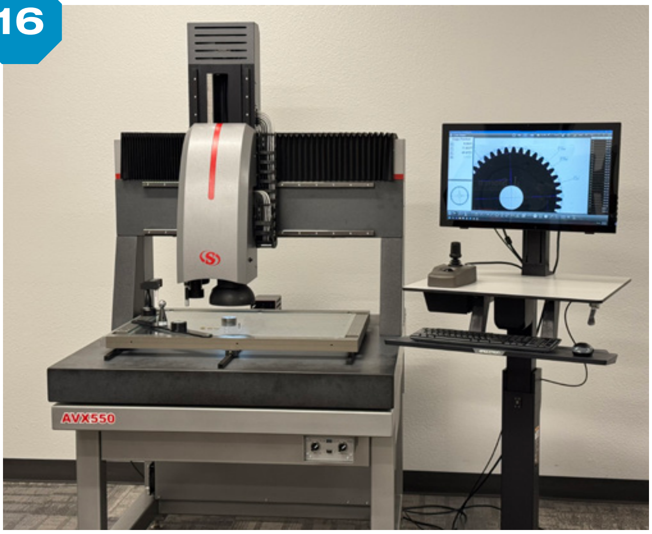

technical

38

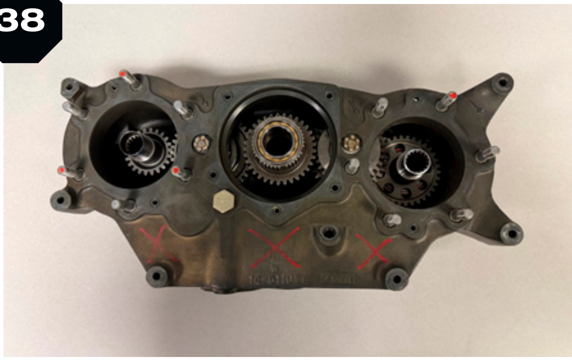

Stay Connected

gt Subscribe Online ***geartechnology.com/subscribe.htm***

Join the Gear Technology Facebook group at ***facebook.com/groups/geartechnology***

Connect with us on LinkedIn ***linkedin.com/groups/3893880/***

Vol. 42. No.4 GEAR TECHNOLOGY. The Journal of Gear Manufacturing (ISSN 0743-6858) is published monthly, except in February, April, October and December by The American Gear Manufacturers Association, 1001 N Fairfax Street, Suite 500, Alexandria, VA 22314, (847) 437-6604. Periodical postage paid at Arlington Heights, IL, and at additional mailing office (USPS No. 749-290). The American Gear Manufacturers Association makes every effort to ensure that the processes described in GEAR TECHNOLOGY conform to sound engineering practice. Neither the authors nor the publisher can be held responsible for injuries sustained while following the procedures described. Postmaster: Send address changes to GEAR TECHNOLOGY. The Journal of Gear Manufacturing. 1001 N Fairfax Street, Suite 500, Alexandria, VA 22314.

gear TECHNOLOGY®
Vol. 42. No. 4


Registration is open!
Visit MotionPowerExpo.com
INNOVATION ACCELERATED
Super Saver rates available until July 15!
Get your Expo Only pass for only $50
Lowest prices of the year!
MOTION + POWER
TECHNOLOGY EXPO®
October 21-23, 2025
Huntington Place • Detroit, MI
AGMA
American Gear Manufacturers Association®

gear TECHNOLOGY®

GT VIDEOS

Marposs Control 2025

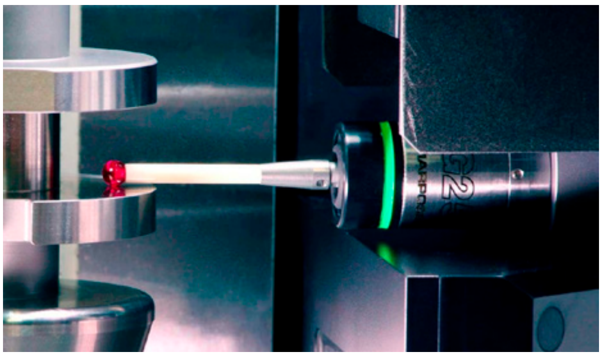

Marposs presents its latest innovations in precision measurement and quality at Control 2025. Marposs technologies support advanced manufacturing processes and ensure the highest standards of accuracy and reliability.

geartechnology.com/videos/marposs-control-2025

Helios Gear Helps American Precision Gear Achieve Quality and Productivity

At American Precision Gear, quality isn't just a priority — it's the foundation of everything they do. The shop specializes in high-precision miniature gears for aerospace, defense, and medical applications, where the strictest tolerances are non-negotiable. Helios Gear Products partnered with American Precision Gear to integrate the MZ 1000 D-Drive into their production.

geartechnology.com/videos/helios-gear-helps-american-precision-gear-achieve-quality-and-productivity

AS SEEN IN *PTE*

Cost-Efficient Manufacturing of Axial Flux Motors

Lambda Resins isn't a typical industry giant – and that's precisely its strength. As a highly specialized resin manufacturer, the company has emerged over the past two years – under the umbrella of Nagel Technologies GmbH – as a sought-after technology partner for OEMs and innovation leaders.

powertransmission.com/cost-efficient-manufacturing-of-axial-flux-motors

AGMA Media
1001 N. Fairfax Street 5th Floor
Alexandria, VA 22314
Phone: 847-437-6604 | Fax: 847-437-6618

EDITORIAL

Publisher & Editor-in-Chief
Randy Stott. Vice President Media
stott@agma.org

Senior Editor
Matthew Jaster
jaster@agma.org

Senior Editor
Aaron Fagan
fagan@agma.org

Technical Editors
Robert Errichello. John Lange. Joseph Mihelick. Charles D. Schultz. P.E.. Mike Tennutti. Frank Uherek

GRAPHIC DESIGN

Design Manager
Jess Oglesby
oglesby@agma.org

ADVERTISING

Associate Publisher & Advertising Sales Manager
Dave Friedman
friedman@agma.org

Manager, Member Engagement and Sales
Katie Mulqueen
mulqueen@agma.org

Materials Coordinator
Dorothy Fiandaca
fiandaca@agma.org

CIRCULATION

Circulation Manager
Carol Tratar
tratar@agma.org

MANAGEMENT

President
Matthew E. Croson
croson@agma.org

FOUNDER

Michael Goldstein founded *Gear Technology* in 1984 and served as Publisher and Editor-in-Chief from 1984 through 2019. Thanks to his efforts, *the Michael Goldstein Gear Technology Library,* the largest collection of gear knowledge available anywhere, will remain a free and open resource for the gear industry. More than 40 years' worth of technical articles can be found online at *geartechnology.com.* Michael continues working with the magazine in a consulting role and can be reached via e-mail at *mwg42@hotmail.com.*

THE GEAR INDUSTRY'S INFORMATION SOURCE

Me Time for Gear Nerds

These days it's really hard to get a break from the cacophony. Our phones are constantly chirping, dinging and lighting up with notifications about the latest, most important thing that we absolutely must see, which leads to scrolling to the next thing…and the next.

We've empowered all our communication platforms to interrupt us and deliver a constant stream of videos, messages and reminders. Much of it is drivel, powered by algorithms that cater to our limited attention span and dwindling expectations for what constitutes entertainment or news value. But much of the digital onslaught is also work-related, generated by the very tools that are supposed to make us more productive.

As a media company, I acknowledge that we're part of the problem.

But at the same time, as a publisher of printed magazines, I would argue that we can also be a part of the solution.

Many forms of art and philosophy emphasize the significance of empty space. In music, the rest between notes can be as important as the notes themselves, adding depth and rhythm. In visual arts, the negative or white space is often what drives the success of a design. Great orators use the dramatic pause to focus your attention.

Anyway, you get the idea. Sometimes you need to manufacture the break. So close your laptop and turn off your phone. Take a vacation. Go sit on the beach. Find a bench in the park. Engage in your favorite hobby or passion.

And if your passion is gear manufacturing, take along your printed copy of *Gear Technology*. While it doesn't provide the escapism of a trashy novel, I guarantee that you'll be rewarded by spending some quality time with one of your favorite subjects.

If you're not currently receiving the printed copy, we can fix that. Go to *geartechnology.com/subscribe* to renew with print, digital or both options.

P.S. If you happen to take my advice and bring your copy of *GT* to a peaceful location, please turn your phone back on long enough to send me a selfie at *stott@agma.org*. We'll make sure we ping your friends with it!

Publisher & Editor-in-Chief
Randy Stott, Vice President Media


Nidec
The Right Machine.
Right Now.
Gear Hobbers • Gear Shapers • Gear Grinders
GEAR MACHINES IN STOCK
Scan to visit our website
VISIT OUR WEBSITE OR CALL US TODAY!
NIDEC MACHINE TOOL AMERICA can also assist with leasing and financing.
www.nidec-machinetoolamerica.com | Call Scott Knoy 248-756-5017
LEGENDARY RELIABILITY
DID YOU KNOW we can also help with...
ADDITIVE MANUFACTURING
Learn more at:
www.nidec-machinetoolamerica.com
BROACH MACHINES AND TOOLS
Visit our website:
www.federalbroach.com
GEAR CUTTING TOOLS AND SERVICE
Send a quote request to:
rfq@federalbroach.com

Siemens and Kuka

OFFER AUTOMATION SOLUTION FOR JOB SHOPS

Siemens offered a new automation solution for the multi-tasking job shop during Automate 2025 in Detroit. The demonstration involved a digital twin of the software and programming of Sinumerik 828 CNC, working in tandem with a Kuka robot, to simplify the operation and programming in part handling for the operator.

Advantages of this development include integrating the robot's programming and operation in the Sinumerik 828 control on one screen, using NC G-code and robot teach-in function for programming, diagnostic data shown on the NC's diagnostic screens allows for the entire automation cell to be monitored and the robotic integration can be tested in Sinumerik 828D's digital twin software, *Run MyVirtual Machine*, while cutting.

As automation continues to impact the machine tool industry, robots and CNC machines are collaborating even more closely. The number of handling and machining robots (machine tools with robotic kinematics) is continually on the rise and Siemens is leading this movement, as the only automation manufacturer in the world that equips its CNC with the necessary interfaces for robotic integration.

Increasingly more machine shops and operators are seeing that automation is an important asset when striving to achieve consistent workpiece quality and more flexibility on the shop floor. Digitalization facilitates the higher level of automation needed and the networking of the components involved. With this new development, Siemens is offering a cost-effective solution that incorporates the KUKA robot functionality with a line of affordable machine tools, in this case, the SYIL brand of machining centers and lathes for small to medium job shops.

As Tiansu Jing, product manager, Sinumerik CNC systems, explains, "The benefits of this development for the busy job shop are many. Setup, programming, operator interface and diagnostics are all improved with this system, as it easily incorporates the Kuka robot with the machine tool." The teach-in functions are implemented through the Sinumerik Operate system on the control, while the proprietary *Sinumerik Run MyRobot* capability of the CNC seamlessly integrates with the Kuka robot control. He further noted that, since there is no need to learn robotic programming, start-up time is reduced and the robot's separate control pendant is eliminated, making the operator's task simplified. The Sinumerik CNC's HMI is used to operate both the machine tool and the robot.

From the Kuka perspective, Ron Bergamin, key technology manager, machine tool automation, comments, "Kuka offers machine tool builders and

end-users alike the ability to incorporate advanced robotics into their equipment and onto their shopfloors, with the goal of optimizing productivity and reducing operator workload. Our partnership with Siemens has resulted in the synergy that brought this development to life. It substantially expands the ability of the small and medium-sized shops to utilize robotics in their work environment."

kuka.com

siemens.com

Schunk

PROVIDES DIGITAL ENGINEERING TOOLS FOR PRODUCTIVITY

The Industrial Metaverse streamlines and accelerates industrial processes. By utilizing digital twins and the use of artificial intelligence, automation tasks can be digitally planned, simulated, and optimized before their physical implementation. Schunk is enhancing its portfolio with digital engineering to unlock new potentials and boost customer productivity.

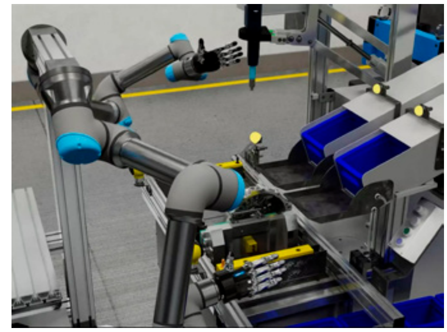

Industry faces the challenge of producing responsibly, flexibly, and efficiently. The development of new products and the necessary manufacturing concepts must now be implemented much faster and be adaptable to variants and variables. The industrial metaverse creates a virtual, interoperable digital space for this purpose. Here, automation concepts can already be planned, extensively tested, and optimized—much faster and more comprehensively than would ever be possible in the real world. Virtual simulation not only accelerates the development of new products and systems but also reduces commissioning times, production interruptions, and costly post-corrections. Schunk also utilizes this to develop new digital components, and to drive technological progress in all areas of automation.

At the core of every simulation is the digital twin—a virtual representation of a physical object or process. This model enables real-time simulation of new workflows and interactions among various process components. Schunk employs a five-stage approach in developing accurate digital twins. Each stage progressively refines components and assemblies from clamping, gripping, and automation technology to closely mirror their physical counterparts. These digital twins encompass not only electrical properties and interfaces but also physical behaviors such as force, friction, and wear. The company has successfully digitally modeled the complete physical behaviors of several products, including new mechatronic parallel and centric grippers. A significant advancement is Schunk's AI-supported 2D Grasping Kit, which automates repetitive sorting and handling tasks. This kit comprises a camera with lens, an industrial PC, AI software, and an application-specific gripper, facilitating reliable handling of randomly arranged parts even under varying conditions. The 2D Grasping Kit's innovative design earned it the prestigious Hermes Award at Hannover Messe.

"By simulating automation tasks, we offer them a highly refined and highly productive solution, quickly optimized for their manufacturing requirements," says Timo Gessmann, CTO of Schunk. "Thanks to AI, we can greatly simplify engineering. With digital tools and simulations, all variants can be validated digitally in no time." In developing digital services, Schunk relies on technology partnerships. For example, the company uses tools like ISG Virtous or Nvidia Omniverse for simulating and planning complex automation projects. Partnerships like the one with Nvidia serve as a catalyst for developing AI-based solutions in simulation and production optimization. Through simulations in the Industrial Metaverse, Schunk creates synthetic data to support the training of AI models.

At the Nvidia GTC in March 2025, Schunk and Schaeffler presented a jointly developed simulated assembly application in robotics, where the 5-finger hand SVH, developed by Schunk, screws components into a housing. The application demonstrates how the boundaries of intelligent automation can be expanded and leveraged for industry. Schunk offers suitable end-of-arm components for all types of robotics, from industrial robots to cobots and humanoid robots, as well as the open digital building blocks for these applications.

schunk.com

B&R Automation

ADDS PLUG-AND-PLAY SCARA ROBOTS TO LINEUP

With the new Codian SR, B&R adds SCARA kinematics to its Codian portfolio of open robot mechanics and integrated machine-centric robotics solutions. The new series offers high-speed articulated movement with four degrees of freedom—perfect for tasks like pick-and-place, loading and unloading, assembly and dispensing that demand both speed and repeatability on a compact footprint.

Complementing the existing Codian delta linup, the new SCARA models extend the range of applications to include high-speed handling with a lateral offset or overhead mounting restrictions. They are particularly easy to install on a small footprint alongside linear and planar product transport systems and handle payloads ranging from 3-65 kilograms with exceptionally high repeatability. The Codian SR lineup includes cleanroom-qualified models that provide compact high-performance handling with undisturbed airflow in sensitive environments like semiconductor or pharmaceutical production.

To ensure maximum flexibility, B&R Codian SR models—like their delta cousins—are available either as open robot mechanics or together with B&R controls and software as an integrated Machine-Centric Robotics (MCR) solution. "Our MCR solutions make robots a plug-and-play part of the machine—physically, logically, and operationally," explains Dario Rovelli, B&R's global product group manager for mechatronics. "That means no extra controllers, no engineering silos—just one seamless system from transport to handling. All thinking and acting as one, in tight synchronization with AI-enhanced machine vision and motion control."

The new SCARA models are also integrated in B&R's open software platform, mapp Robotics, making it easy to incorporate sophisticated robotic handling in the machine application without specialist knowledge in robotics programming. Users have access to all the familiar machine programming languages like Ladder Diagram, Structured Text and C/C++ and ready-made software components needing only configuration and tuning, all in the familiar Automation Studio engineering environment.

"With mapp Robotics and our integrated approach, machine builders can implement robotics applications without needing robotics expertise," says Sebastian Brandstetter, B&R product manager for robotics. "It's about empowering engineers to focus on machine performance and product quality – not on bridging technical gaps between systems."

Unifying machine and robot control reduces complexity and setup time. With preconfigured templates, simulation tools, and standardized interfaces, commissioning is faster and easier. B&R's deep expertise in tuning, synchronization, and motion ensures that the robot performs at its best in the context of the entire machine. It's all part of a seamlessly integrated automation package—spanning software, hardware, and services—from a single source.

br-automation.com

Fanuc

SHOWCASES LATEST INDUSTRIAL AND COLLABORATIVE ROBOT SOLUTIONS

Fanuc America displayed its latest industrial and collaborative robotic innovations at Automate 2025.

"Today, more than ever, automation is the key to reaching production targets, boosting efficiency, and ensuring employee satisfaction," says Mike Cicco, president and CEO of Fanuc America. "From start-ups to large-scale manufacturers, Fanuc provides industry-leading, dependable, and cost-effective automation solutions that help companies overcome their greatest challenges."

At Automate, Fanuc offered a broad selection of new and innovative technologies including a full line of collaborative robots—or cobots—featuring payloads of up to 50 kg and reach at 1,889 mm. Within the diverse cobot selection, Fanuc also showcased its CRX-10iA/L Paint Cobot specifically designed for use in painting, coating and dispensing.

Mounted on a third-party autonomous mobile robot, Fanuc's CRX-10iA/L Cobot demonstrated automotive kitting as it used the iRVision 3DV vision sensor to accurately pick individual components of a vehicle side-view mirror and deliver the kit to a human operator for assembly and installation onto a door, easing the labor process and eliminating the need for manually delivering parts or kits to the assembly line.

Fanuc used two cobots, visual identification and advanced line tracking to identify, load, paint and unload electric guitar bodies. Using a CRX-10iA/L Paint Cobot with Fanuc 3DV camera and iRVision, the system visually tracked and simulated painting of the guitar bodies. Meanwhile, a CRX-20iA/L Cobot loaded and unloaded guitar bodies from a conveyor to a rack.

Fanuc's Integral Servo Dispenser Software is paired with adhesive metering equipment to deliver a mobile dispensing system featuring more precise application, better control, better repeatability, and intuitive programming. In this demonstration, a Fanuc CRX-30iA cobot featured end-of-arm adhesive metering, Fanuc 3DV/400 vision camera and SpotTool+ software to offer a reliable, repeatable, and easily programmable dispense solution in a compact and flexible footprint.

In a two-station cell, Fanuc demonstrated the flexibility and increased productivity allowed when its CRX-10iA/L Cobot is integrated with a 7th axis rail. Featuring a single-axis positioner on one side and a flexible fabricating table on the other, an operator can easily load one cell while welding occurs at the other thanks to an increased work envelope.

Fanuc's high-precision M-800/60-20B industrial robot milled and drilled aluminum stock using a variety of tools and accommodating various mounting positions. Built to withstand harsh elements like water and debris, this 6-axis model, known for its rigidity and accuracy, offerred a larger work envelope compared to similarly priced CNC machines. Additionally, its adaptability makes it suitable for repurposing across various applications.

The compact LR Mate/7-7D robot with Fanuc's 3DV/400 vision camera bin picked jumbled boxes from a container onto a conveyor. This robot is running python code natively on its paired Fanuc controller. The second robot, LR Mate/7-9 long arm unit with a 3DV/400 camera and PalletTool Turbo II software—identifies the size of the box on the conveyor and palletizes it onto the appropriate pallet. This controller showcases new cybersecurity protocols including MQTT TLS, the use of a LDAPS server for user access control along with Software PLC capability for cell control and HMI functionality. Additionally, Teach Pendant with lighter weight and enhanced performance is featured.

fanucamerica.com

Sharper Eyes on Precision Gears

How multisensor metrology is transforming spur gear inspection with integrated vision and tactile probing

Greg Maisch, Engineering Manager, Starrett Metrology Systems Division

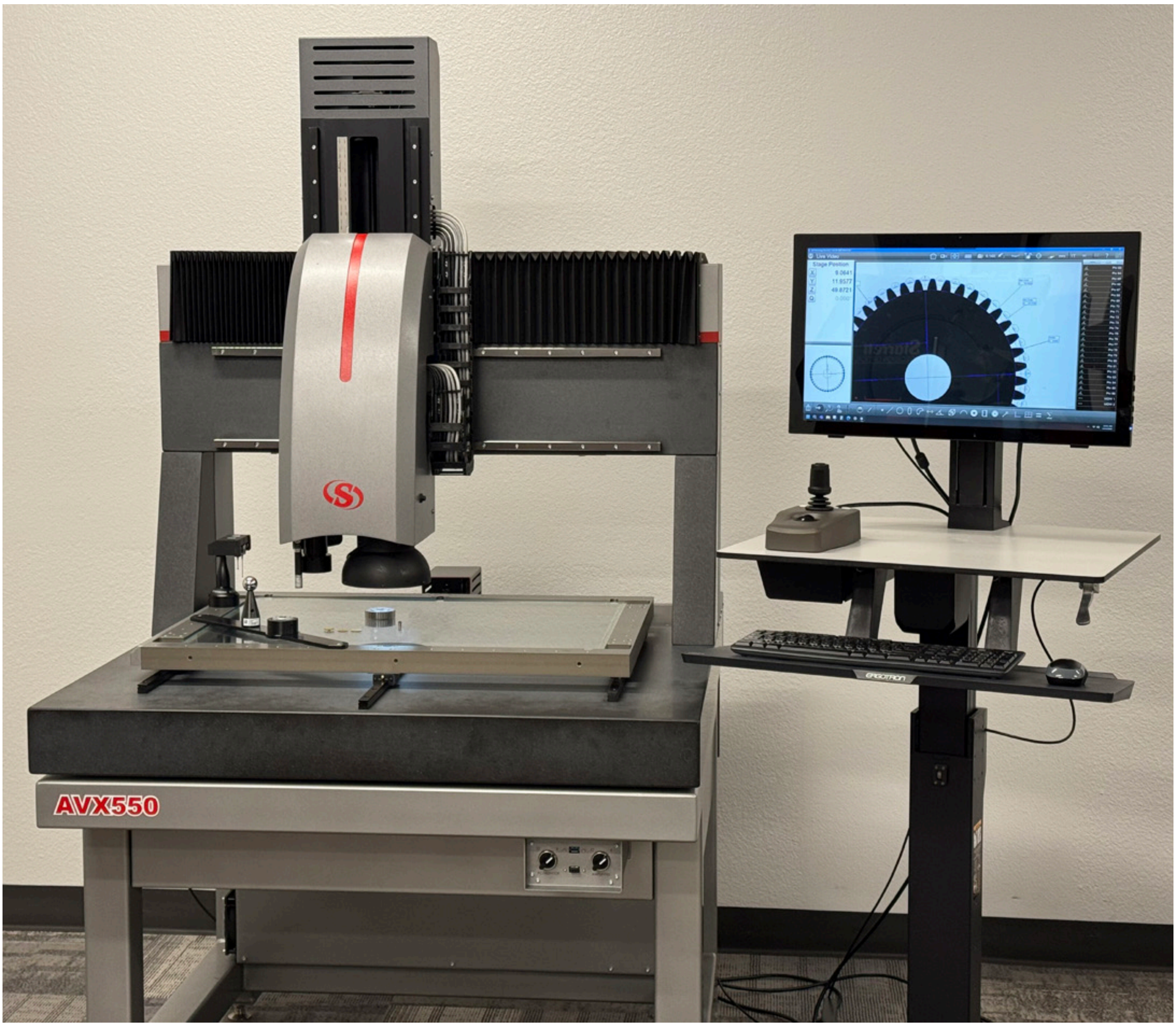

Starrett multisensor metrology system inspecting a spur gear using integrated vision and tactile capabilities. The M3 Gear Module *software enables fast, accurate, and repeatable inspection. (Courtesy of Starrett Metrology Systems Division.)*

In the world of precision manufacturing, the performance and longevity of many mechanical systems are determined by the quality of their gear components. Accurate gear inspection is vital to ensure that these components meet stringent design specifications and functional performance requirements. However, traditional tactile-based inspection methods can be time-consuming, labor-intensive, and prone to variability, especially as production volumes and complexity increase.

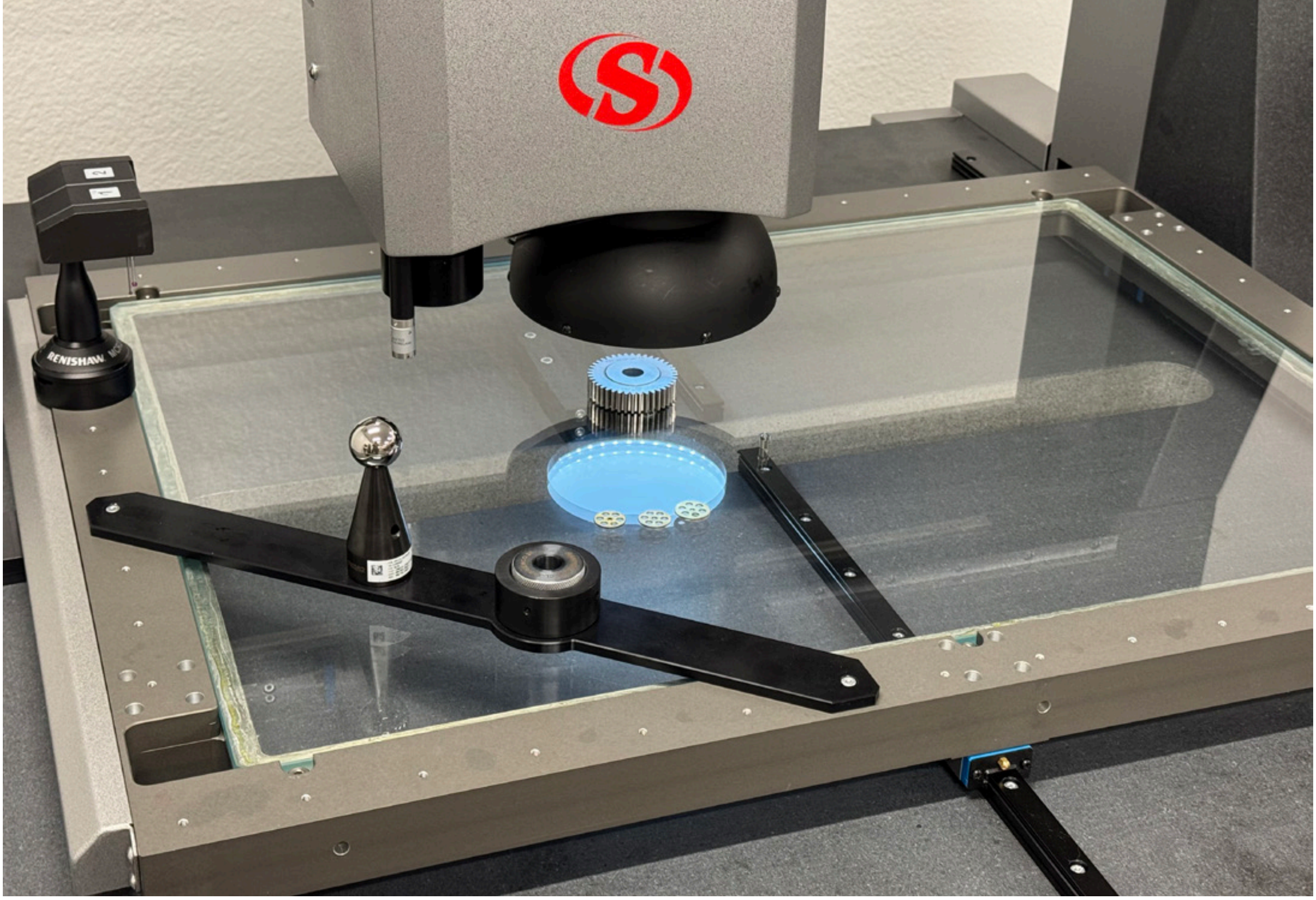

Close-up of spur gear under high-resolution camera. Vision-based edge detection rapidly captures critical geometric features without physical contact. (Courtesy of Starrett Metrology Systems Division.)

Recognizing the need for a faster, more reliable approach has prompted a new gear inspection solution that combines advanced vision-based measurement with tactile touch-probe capabilities. Central to this is the integration of the *M3 Gear Module*, developed by MetLogix, along with multisensor metrology systems from inspection equipment manufacturers such as Starrett. The combination offers gear manufacturers and users an efficient, accurate, and repeatable solution for inspecting spur gears that streamlines inspection workflows while ensuring compliance with industry standards.

Using automated edge detection in combination with preprogrammed macros, this solution substantially increases the efficiency with which spur gears are measured via parameters such as maximum/minimum gear diameter, gear tooth width, master gage circle diameter, measurement over simulated/theoretical wires (MOW), and phi angles. In addition to these specific gear measurements, the system can be used to check tooth profiles as well as features that can only be gathered with a tactile probe, such as flatness and planar parallelism. This article explores how the integrated approach enhances both production throughput and quality assurance, providing significant value to manufacturers across a range of industries.

Traditional Impediments

Conventional gear inspection methods have traditionally relied on measurements using hand tools, tactile probing systems, and custom mechanical measurement devices to verify gear geometry. While effective, these methods present several challenges, particularly as demands for higher production speeds and tighter tolerances continue to grow in manufacturing.

Hand tool and tactile-only inspection processes are inherently time-consuming, requiring physical contact with each gear tooth or surface. As a result, the measurement cycle can become lengthy. In addition, the quality of the measurement often depends heavily on operator skill and consistency, introducing potential sources of variability into the inspection process.

Another limitation of tactile methods is the inability to rapidly capture the data for all of the teeth on the gear; thus, these processes generally result only in the spot checking of a few key areas. Physical quality checks, while precise, are constrained in their ability to quickly scan complex surfaces without risking potential wear or damage to delicate gear features or the equipment used for checking them. These constraints make traditional inspection methods less suitable for high-volume manufacturing environments where efficiency, repeatability, and minimal part handling are critical.

Advancements Through Vision

Advancements in optical measurement technology have opened new possibilities for gear inspection, offering significant advantages over traditional tactile approaches. Vision-based inspection systems utilize high-resolution imaging, sophisticated edge detection algorithms, and automated feature recognition to rapidly capture precise measurements without physical contact. This capability enables manufacturers to significantly reduce inspection cycle times while enhancing data reliability and repeatability.

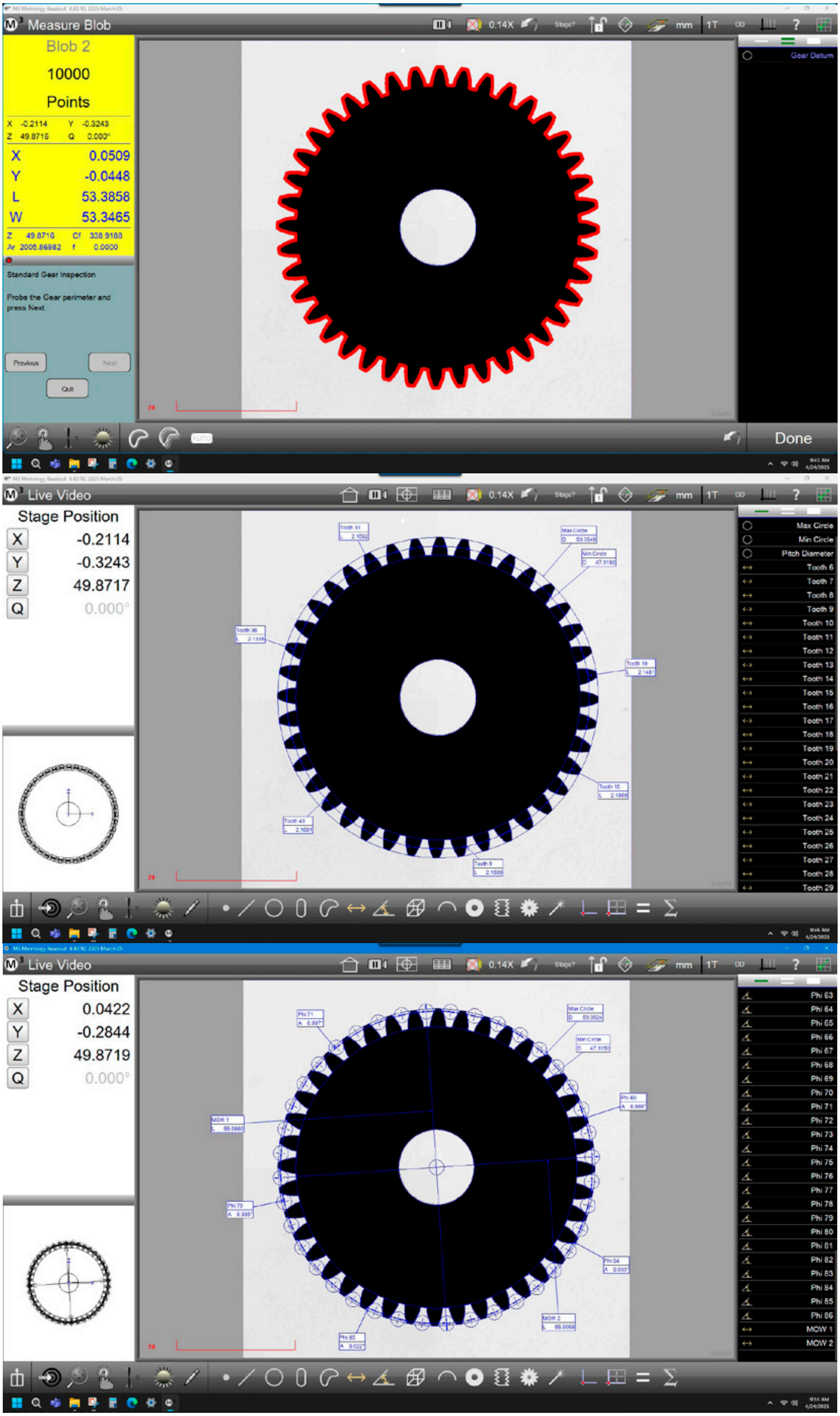

Captured inspection data from over 10,000 points enables comprehensive gear analysis. M3 Gear Module software evaluates key parameters such as tooth width, phi angles, and diameter tolerances with visualized results for fast decision-making. (Courtesy of Starrett Metrology Systems Division.)

Using multisensor metrology systems integrated with the *M3 Gear Module*, spur gears can all be measured with exceptional speed and precision. By analyzing captured images with high-resolution imaging, the system automatically identifies and evaluates gear features, eliminating the need for extensive manual programming or intervention.

Non-contact vision systems also minimize the risk of part damage, making them ideal for inspecting delicate or finely finished gear components. Moreover, the ability to visualize and archive inspection data enhances traceability and facilitates more comprehensive quality reporting.

In high-volume production settings, the benefits are even more pronounced. Automated vision inspection reduces the reliance on operator skill, ensuring consistent, repeatable results across shifts and production runs. It also enables real-time feedback into manufacturing processes, supporting more proactive quality control and continuous improvement initiatives, combining increased throughput, efficiency, accuracy, and flexibility into a single, integrated solution.

Software for Spur Gear Measurement

At the heart of the inspection system is the *M3 Gear Module*, a comprehensive, intuitive software extension designed specifically for the measurement of spur gears. The module provides a range of capabilities that substantially streamline the inspection process while delivering highly accurate and repeatable results.

The module features an extensive suite of measurement functions, enabling users to evaluate critical gear characteristics. By using advanced video edge detection and intuitive workflows, users can complete complex inspection routines quickly and with minimal training.

To further enhance efficiency, the module includes predefined "Standard" and "Master" inspection macros. These macros guide operators step-by-step through the measurement process, ensuring consistency and reducing the potential for human error. Once the measurement sequence is completed, results are generated instantly and presented in clear, easy-to-read data views.

The module also provides very effective visualization tools. Gear tooth width and phi angle results can be displayed in customizable bar graphs, allowing operators to immediately identify deviations from specification.

A unique feature of the module is its seamless integration of nominal values, tolerances, and result statistics. Using its tolerance system, operators can quickly apply limit values and generate detailed statistical summaries, including minimum, maximum, range, and average measurements. The system also supports the application of concentricity and runout tolerances, enabling an in-depth evaluation of gear quality in a single, automated routine. Measurement data can then be exported in a variety of ways, and reports can be customized to conform to the reporting standards of the manufacturer.

By integrating these capabilities into an intuitive, touchscreen-driven interface, the module enables manufacturers to significantly reduce inspection cycle times while improving repeatability, traceability, and compliance with demanding industry standards such as ISO 1328 and AGMA 2015.

The integration of the *M3 Gear Module* with Starrett's multisensor metrology systems significantly enhances inspection efficiency and measurement precision. By automating complex measurement routines and reducing manual intervention, manufacturers can achieve faster inspection cycles and consistent, high-quality results, ensuring compliance with stringent industry standards.

Tactile and Touch Probing—A Hybrid Solution

While vision-based inspection offers rapid and comprehensive data capture for two-dimensional features, there are situations where tactile probing remains essential, particularly when inspecting three-dimensional geometries that are not accessible optically. Recognizing this, Starrett multisensor metrology systems offer touch-probe capabilities alongside vision measurement, offering a hybrid inspection solution.

The combination of vision and tactile probing allows for more complete characterization of spur gears, ensuring that both 2D and basic 3D features are accurately measured. Vision systems are very effective at capturing critical features that can be projected as a plane, such as tooth spacing, involute profiles, and lead angles with exceptional speed. When deeper geometries or form features—such as bores, cones, or datum planes—require measurement, the system can automatically transition to tactile probing.

Although the *M3* platform is not designed for direct 3D CAD model comparisons or full 3D surface profiling, it does provide extensive tactile measurement capabilities. The touch probe can accurately measure discrete geometric features, including points, lines, planes, spheres, cylinders, and cones. Dimensional and geometric tolerances such as parallelism, perpendicularity, concentricity, and runout can be applied to these features, supporting comprehensive inspection needs.

This hybrid approach increases measurement flexibility while enhancing overall inspection efficiency. Operators can define inspection routines that intelligently deploy vision and tactile methods based on feature accessibility and tolerance requirements. Results from both modalities are combined within a single software environment, simplifying data reporting and ensuring full traceability.

By blending the strengths of high-speed optical measurement with precision tactile probing, these hybrid metrology systems deliver a versatile solution capable of addressing the diverse challenges of modern gear manufacturing.

This approach not only reduces inspection cycle times and training requirements but also enhances measurement repeatability and traceability.

As gear designs become more complex and production demands rise, multisensor inspection systems like these will be critical in ensuring consistent, high-quality output—delivering a competitive edge to manufacturers in precision industries.

starrettmetrology.com

For Related Articles Search
inspection
at geartechnology.com

Smarter Clamping Starts at the Core

Discover how Gleason's reengineered segmented collets optimize ID workholding with advanced materials, broader expansion ranges, and proven long-term durability

Robert Peyr, Director Product Management, Global Services and Workholding, Gleason Corporation

Modular workholding device with segmented collet.

Benefits

- Industry standard, compatible with most common workholding devices.
- Standard version from 20–120 mm in very fine increments of 0.25 mm.
- Large expansion areas thanks to highly flexible vulcanization between the segments.
- Vibration damping through vulcanized segments.
- Concentricity accuracy of ≤ 0.005 mm.
- Pull back feature to ensure positive seating.
- Auto load compatible.

The latest generation of segment collets from Gleason ensures exceptionally accurate and reliable clamping in the part bore, while the new segment clamping sleeves' universality enables clamping a wide range of components.

Flexibility Is Key

Adaptability and flexible production are now possible even for small batch sizes. The frequent changeover between workpiece types shows the weaknesses of conventional fixtures for clamping on the inside diameter, which are often not flexible or sufficiently reliable.

Workholding systems that use segmented collets that expand to exert a centering and clamping effect in the diameter of the workpiece bore are among the best solutions available for flexible production environments. Workholding systems with segmented collets show their strengths equally with small batches and a large variety of parts. As a single collet can accommodate a whole range of different bore diameters within its clamping range, its use results in greater flexibility and simultaneous cost savings, as both equipment costs and non-productive times are reduced almost automatically.

Segmented collets usually consist of an assembly with segments made of high-strength steel, which are joined with vulcanized high-tech elastomer using an injection molding process. This combination provides a larger expansion range than steel alone and also dampens vibrations. The expansion (chucked) or contraction (de-chucked) of segmented collets is usually carried out with an expander, which is actuated by a draw rod within the production machine. When the drawbar is actuated, the expander causes the segmented collets to expand and exerts a particularly rigid clamping effect via the end face, respectively, a pulling effect on the workpiece.

Blue Means Precision

Gleason segmented collets are recognizable by the typical blue color of the high-tech elastomer and can be used on workholding devices from all common manufacturers. The standard product line of segmented collets covers a range from 20–120 mm in fine increments of 0.25 mm, with an excellent concentricity of ≤ 0.005 mm. Additionally, Gleason manufactures clamping collets according to customer specifications on request.

Reliability Rethought

To minimize or ideally eliminate the occurrence of excessive wear, fatigue and runout, Gleason segmented collets are designed from the ground up: In addition to finite element analysis, the most rigorous life cycle testing using specific test fixtures is employed to perform actual chucking/de-chucking cycles of the prototypes, simulating many times the average life expectancy of a segment collets—with more than 1 million clamping cycles. The results of the long-term tests speak for themselves: No signs of fatigue with a constant concentricity error of ≤ 0.005 mm.

gleason.com

For Related Articles Search
workholding
at geartechnology.com

The Hazards of Heavy Lifting

DBS Canada repairs mobile mining gearbox for iron ore application

Matthew Jaster, Senior Editor

David Brown Santasalo's range of shovel and dragline transmissions for the mobile mining industry are available as complete assemblies or as replacement components.

A rope shovel is a bucket-equipped machine used for digging and loading earth or fragmented rock. Rope shovels are a type of rope/cable excavator, where the digging arm is controlled and powered by winches and steel ropes, rather than hydraulics. In mining applications, the rope shovel distributes materials such as iron ore into larger-than-life dump trucks. David Brown Santasalo (DBS) Canada delivers an extensive range of gear systems for shovels, draglines and other surface mining equipment.

Last year, DBS Canada's manufacturing facility in Montréal completed the repair of a mobile mining gearbox for a customer in the iron ore industry. This was a huge achievement for DBS Canada. The 27-ton gearbox required a complete refurbishment, consisting of new bronze bearings and roller bearings, renewed housing bores, new gears and pinions with DBS optimized geometry.

For Related Articles Search
off-highway
at geartechnology.com

Heavy Mobile Equipment

"We're always focused on critical gearboxes," said Steven Bednarchuk, technical sales support, DBS Canada, "and we're well known for making really good gear repairs, for instance, on stacker reclaimers in the iron ore industry."

Bucket wheel reclaimers are large machines used in material handling, particularly in mining and bulk material storage. There are various types, including bridge-type and boom-type bucket wheel reclaimers, which are suited for different applications such as coal, iron ore and other bulk materials.

"These bucket wheel gear drives are very complex units, and our customers don't want to risk anything or cut corners when it comes to the quality and viability of the equipment," Bednarchuk said. "Since we have the capability to manufacture our own products and we're very meticulous about the teardowns and analysis of our units, we have a very good nonreturn rate. The gearbox comes out of our facility almost brand new."

The DBS Canada team gains a deeper understanding of these applications with each new project. "Our end goal is to ensure these repairs are done right the first time," Bednarchuk said. "The equipment's condition coming in for repair has proven that these markets have not been served very well for a long time. Many shortcuts were taking place—particularly in the gearboxes operating the boom on the rope shovels."

Like many heavy industrial applications, weight distribution during assembly and disassembly remains a critical challenge. The weight of the large gears and components are removed/added 1 by 1, thus shifting the center of gravity/weight around of the crowd unit, making it dangerous to work on because it wants to tip over.

Meeting strict deadlines can also be a challenge in these industrial applications.

"A short timeframe is requested, but it's in the customers best interest to make sure the gearbox rebuild or refurbish is done correctly," Bednarchuk said. "We're honest about what needs to be done within the gearbox system and the timeframe it may take. All the gears in this application, for example, needed to be replaced."

Cracks that were detected within the enclosure by Non-Destructive Testing (NDT) were also restored. Once complete, DBS conducted a spin test performed with vibration analysis, to ensure the gearbox repair was delivered to the highest standards, ready to return to operating the electric rope shovel.

"Ultimately my emphasis was on quality. Also, the fact we were going to spin test the unit gave the customer additional protection. These were steps our customer did not receive in the past. Typically, the unit was simply put together, sent to the site and installed," Bednarchuk said.

Without spin tests or vibration analysis, a mining customer could discover faults or anomalies after the installation resulting in weeks of additional downtime.

Enhanced Product Portfolio

David Brown acquired Unigear—based in Montreal—in 2012. Today, DBS Canada provides key gearbox services and support across several industries including mining, oil and gas, cement, metals, power generation, rail and more with an emphasis on quality, reliability and longevity.

The DBS Canada team responsible for rebuilding the rope shovel gearbox. Left to right: Kerolos Boulos, Paulo Rodrigues, Steven Bednarchuk, Patrick Morin and George Rodrigues.

The acquisition of Unigear provided David Brown with wider access to many of these strategic industry segments coupled with local capability to manufacture and service industrial gear products for the North American market. Thanks to a combination of customer relationships, experience, skills and precision gear manufacturing equipment, DBS Canada offers localized service and support throughout the region.

The company's global work in heavy mobile equipment—particularly in areas like Chile and Australia have been extremely valuable for DBS Canada.

"They have all the drawings; all the technical knowledge and engineering support we need to better assist our customers here in Canada," Bednarchuk said.

From Refurbish to Rebuild

Being a gear manufacturer, DBS has gear grinders on-site. "As these projects come into the shop and we find superficial micropitting on the gear teeth, we can kiss grind the gears and renew the integrity of the components. This can save our customers a lot of money," Bednarchuk said.

"We invited the customer into the shop so they could better understand the repairs needed," Bednarchuk said. "These gearboxes are known to be the weak link in the system because they work so hard in the application. Our focus on the project led to the customer sending us another high value gearbox for additional repair services."

The Power of Predictive Maintenance

Everyone is banking on predictive maintenance and hoping to stay ahead of critical failures in mining, off-highway and processing applications.

Bednarchuk sees predictive maintenance, sensors and IIoT taking a much larger role in gearbox applications.

DBS has their own software for predictive maintenance, known as *GearWatch*. The software ensures the gearbox is running effectively and will warn the customer if something is not working correctly, signs of deterioration, etc. It measures, records and analyses data, reporting changes in measured parameters in real time, 24/7 via the internet. Not only does it measure changes within the gearbox, but it can also monitor a full range of equipment including motors, hydraulic systems and bearings.

Real time information transmission enables quick recognition of problems, meaning fast corrective action is taken before downtime occurs. The system is constantly observing process parameters and equipment operation online.

Labor shortage is everywhere. The future of gearbox production is going to be customers looking at drop-ins more than anything else, according to Bednarchuk.

"They want to eliminate the work onsite due to the lack of time, knowledge and available engineering expertise. This is the direction the industry is heading. These drop-in units where everything has been rebuilt and they're simply plug and play. The customer can install the unit and not worry about it."

dbsantasalo.com

WGT 1200 Optimized for Automatic Loading of Large Workpieces

High-precision measuring machines for small and large gears

High-precision measurements even with heavy styluses.

For Related Articles Search
measurement
at geartechnology.com

The Liebherr WGT series of gear measuring machines is used in gear manufacturing for a wide range of industries: from the smallest aerospace applications to large gearbox components for wind turbines, tower cranes or commercial vehicles, where some of the gears weigh tons. With the optimized WGT 1200, Liebherr-Verzahntechnik GmbH provides high-precision measurement even for huge workpieces up to a diameter of 1400 mm and a weight of 5 tons.

The WGT range of gear measuring machines is suitable for workpieces with diameters from 5–1,400 mm, starting with the WGT 280 followed by WGT 400 up to the recently updated WGT 1200 for workpieces weighing up to 5 tons.

WGT Series for Diverse Requirements and Strict Demands

All the models meet the strict requirements of VDI/VDE 2612/2613, Group 1 and can measure gears from a module of 0.1 mm. The base plate, linear guides and tailstock made of lapped natural granite ensure a constant temperature profile, while linear axes with air bearings, precision rotary tables and reliable Renishaw probe systems with touch probes ensure the mechanical accuracy of the machines. Operation is intuitive using the LHInspect software, which allows the gear cutting machine and the inspection machine to exchange geometrical and measurement data for automatic correction in a closed loop.

An optional, optimized roughness sensor handles even the smallest measuring points. The automatic stylus change rack with up to two six-piece magazines ensures uninterrupted measurement of the workpieces in a single operation. "This makes the measurement not only highly precise, but also efficient and user-friendly," summarizes Matthias Brüderle, product manager for gear measuring machines. Some of the WGT models can be demonstrated in the show rooms in Ettlingen. "We also offer basic and advanced training courses by experienced trainers—on our customers' own workpieces if they wish," says Brüderle.

WGT 1200: Swiveling Upper Center, Reduced Footprint

The concept of the largest measuring machine, the WGT 1200, has now been revised and optimized. "We benefited from our experience with gear cutting machines, from which we adopted the concept of the tailstock. It is now permanently installed and the upper center swivels sideways," explains Brüderle. This arrangement increases the load area and also saves space. What is particularly interesting is that this makes the WGT 1200 suitable for automatic loading by robots and automatic clamping, which means it is prepared for unmanned operation.

The WGT 1200 in a new design with a swiveling tailstock.

Another highlight of the WGT 1200 is the powerful spindle drive, which ensures optimized power transmission, precise positioning and high load capacity. The machine is also equipped with active damping, which eliminates the need for a separate machine foundation. The Renishaw SP80 probe can also support heavy styluses while maintaining the highest degree of accuracy. The current version of the WGT 1200 was presented to visitors at the international trade fair Control in Stuttgart in May, where it attracted a great deal of interest.

liebherr.com

Emerging Technologies in Transition: Forecasting the Future of Automobile and Humanoid Robots

Mary Ellen Doran, AGMA Vice President, Emerging Technology

In our two most recent emerging technology webinars, we examined two sectors undergoing transformative shifts—the automobile industry and robotics, specifically electric vehicles (EVs) and humanoid robots. The auto industry shifted focus to EVs a few years ago, and more recently, there has been growing momentum in humanoid robot development. These technologies have generated significant press and investment. Each presenter helped separate fact from fiction in these evolving spaces.

Our April presenter, industry veteran Joe McCabe, provided insights into the global and North American automotive markets, drawing from his firm's comprehensive forecasting models. His firm forecasts every vehicle produced globally over the next decade. While much attention has been given to government regulations and environmental mandates promoting EV adoption, McCabe emphasized that consumer demand remains the ultimate market driver. He outlined global light vehicle production—where the industry was, where it is today, and where he sees it going.

He focused on suppliers and industry shifts that will directly impact relationships between suppliers and OEMs. He noted that in North America, 14 vehicle manufacturers produced 17.8 million units in 2016, the highest sales year on record. This year, 24 manufacturers are making fewer units, and his forecast shows 28 manufacturers in play by 2031. Pricing can no longer remain as it was; everything will cost more. The impact is already being felt—16 vehicle programs have been moved out of the forecast to 2028 and beyond, with production not returning to 2016 levels. McCabe also shared insights on specific vehicle programs, tariffs, and other key market factors.

In May, Ruben Scriven, leader of the warehouse automation research practice at Interact Analysis (IA), turned the spotlight on robotics, particularly the recent surge in humanoid robot interest. Despite increased investment and media attention in 2024 and 2025, Scriven was quick to temper expectations.

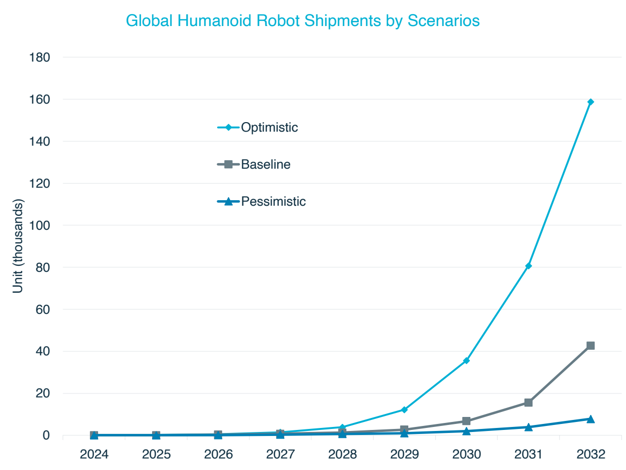

Source: Interact Analysis, *Humanoid Robots–2025*

He shared findings from IA's March market study, "Humanoid Robots—2025: A pragmatic assessment of the potential and likely future development of a nascent market." He noted that in the current climate, insurers are hesitant to provide coverage for humanoid robots due to a lack of technical specifications and an immature regulatory framework. He also pointed out that not all warehousing and manufacturing roles are substitutable with humanoids—only about 27 percent of U.S. manufacturing roles are technically feasible for replacement. Furthermore, core technical barriers must still be overcome before humanoids can match human dexterity and productivity.

Nevertheless, IA forecasts that by 2032, humanoid robots will be sold in the tens of thousands per year, generating over $2 billion in revenue, with considerable additional potential.

Meanwhile, mobile automation systems—such as autonomous mobile robots (AMRs) and shelf-to-person solutions—are outpacing fixed infrastructure in downstream applications. The warehousing boom sparked by the pandemic has cooled, but optimism is rising in manufacturing automation and reshoring, where robots—humanoid or otherwise—could help address persistent labor shortages.

The message from both webinars is clear: the future is being built—but not without disruption. Companies operating in or adjacent to these sectors must balance innovation with pragmatism and view emerging technologies as part of a longer-term evolution, not a short-term revolution.

The AGMA Emerging Technology committees continue to have high-level discussions on these topics and more. I encourage you to join the conversation. Please reach out to me at *doran@agma.org*. Both webinars discussed in this article are available free, on-demand, on the AGMA website.

agma.org/events-education/on-demand-webinars/

AGMA Historic Accuracy Grades

Phillip Olson, Director, AGMA Technical Services

We get a lot of questions here at AGMA asking for help in decoding gear accuracy grades (also known as tolerance classes). If we're lucky the inspection standard is called out on the print, or the customer knows what standard they want the gears to be inspected, or they are ok to use the most current standard. If that's not the case it takes some detective work to determine the proper inspection standard.

I have a table I use as a first step (Page 31) to decode the different accuracy grade designation systems historically used by AGMA. The current designation systems used are highlighted in the table. Looking at letter designations, year published, or type of gear covered columns can help narrow down what standard the designer was thinking of, as long as it's to an AGMA standard. Tracking down international designations would be another level of complexity. If you need a historic standard to reference for old parts, AGMA maintains an archive of historic standards not on our document store, but available upon email request to *tech@agma.org*.

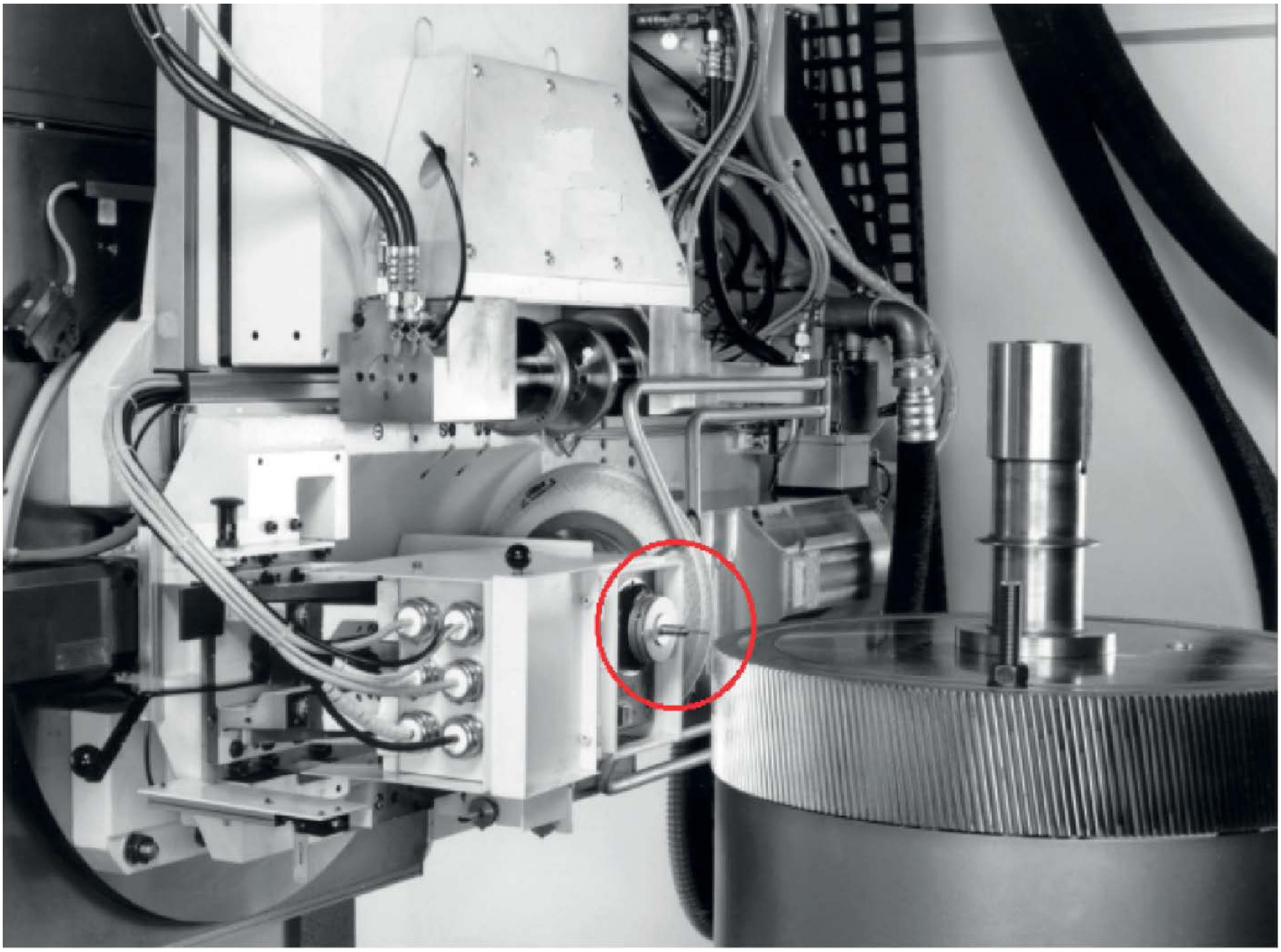

Accuracy Grade Designations	Standard	Year First Published by AGMA	Notes
V3 to V14	AGMA 943-A22	2022	As numbers increase precision decreases Covers rack flank tolerances
R31 to R50	AGMA 943-A22	2022	As numbers increase precision decreases Covers rack composite tolerances
R30 to R50	ANSI/AGMA ISO 1328-2-A21 (Identical to ISO 1328-2:2020)	2021	As numbers increase precision decreases Covers spur and helical composite tolerances
R20 to R30	ANSI/AGMA 2015-2-B15	2015	As numbers increase precision decreases Covers spur and helical composite tolerances
1 to 11	ANSI/AGMA ISO 1328-1-B14 (Identical to ISO 1328-1:2013)	2014	As numbers increase precision decreases Covers spur and helical flank tolerances
2 to 11	ANSI/AGMA ISO 17485-A08 (Identical to ISO 17485:2006)	2008	As numbers increase precision decreases Covers bevel gear tolerances
M1 or M2	ANSI/AGMA 2015-2-A06	2006	M1 is more precise than M2 Method suffix code "T" and/or "R" required Covers spur and helical master gear tolerances
C4 to C12	ANSI/AGMA 2015-2-A06	2006	As numbers increase precision decreases Covers spur and helical composite tolerances
A2 to A11	ANSI/AGMA 2015-1-A01	2001	As numbers increase precision decreases Covers spur and helical flank tolerances
4 to 12	ANSI/AGMA ISO 1328-2 (Identical to ISO 1328-2:1997)	1999	As numbers increase precision decreases Covers spur and helical composite tolerances
0 to 12	ANSI/AGMA ISO 1328-1 (Identical to ISO 1328-1:1995)	1999	As numbers increase precision decreases Covers spur and helical flank tolerances
B3 to B10	ANSI/AGMA 2009-B01, ANSI/AGMA 2009-A98, ANSI/AGMA 2009-B01	1998	As numbers increase precision decreases Covers bevel gear tolerances
3 to 12	ANSI/AGMA 2011-A98, ANSI/AGMA 2111-A98, ANSI/AGMA 2011-B14	1998	As numbers increase precision decreases Covers inch and metric wormgearing tolerances
5 to 1 (Coarse pitch) 4 to 1 (Fine pitch)	ANSI/AGMA 2000-A88	1988	As numbers increase precision increases Tooth thickness code, either "A" or "B" required Text "Master C" required before grade Covers spur and helical master gear tolerances
Q15 to Q3	ANSI/AGMA 2000-A88	1988	As numbers increase precision increases Optional "thickness", "material", and "treatment and hardness" designation codes (Example with optional codes "Q8A-HA14") AGMA 390.03 covers spur, helical, bevel, hypoid, rack and wormgearing tolerances, AGMA 390.03a covers bevel, hypoid, rack and wormgearing tolerances, ANSI/AGMA 2000-A88 covers spur and helical gear tolerances
	AGMA 390.03a	1988	
	AGMA 390.03	1980	
16 to 5 (Fine pitch)	AGMA 237.01	1964	Accuracy specification coding per AGMA 390.02 with addition of an angular tolerance letter code (d to z) As letters approach z precision decreases (Example with angular tolerance code "8-H-14r")
7 to 1 (Coarse pitch) 6 to 1 (Fine pitch)	AGMA 235.02, AGMA 390.3	1964	As numbers increase precision increases Tooth thickness code, either "A" or "B" required Covers spur and helical master gear tolerances
15 to 3 (Coarse pitch) 16 to 5 (Fine pitch)	AGMA 390.02	1964	As numbers increase precision increases Optional "backlash", "material", and "treatment and hardness" designation codes (Example with optional codes "10C-A-4") AGMA 390.01 covers spur and helical gear tolerances, AGMA 390.02 covers spur, helical, bevel, hypoid, and rack tolerances
	AGMA 390.01	1961	
Classes 3 to 1	AGMA 234.01	1956	As numbers increase precision increases Covers wormgearing tolerances
Classes 3 to 1	AGMA 235.01	1947	As numbers increase precision increases Covers spur and helical master gear tolerances
Classes 3 to 1	AGMA 236.01A, AGMA 236.02, AGMA 236.03, ASA B6.11-1951, AGMA 236.04, ASA B6.11-1956	1946	As numbers increase precision increases Covers fine pitch spur, helical, bevel and worm master gear tolerances
Commercial Classes 4 to 1 Precision Classes 3 to 1	AGMA 236.01, AGMA 236.01A, AGMA 236.02, AGMA 236.03, ASA B6.11-1951, AGMA 236.04, ASA B6.11-1956	1945	As numbers increase precision increases Optional backlash designation code (A to D) Covers fine pitch spur, helical, bevel and wormgearing tolerances
Classes 4 to 1 (Spur & Helical) Classes 4 to 2 (Bevel)	ASA B6.6-1946, AGMA 231.01, AGMA 231.02, AGMA 232.01, AGMA 232.02	1943	As numbers increase precision increases Classes divided according to speed Covers coarse pitch spur, helical, and bevel gear tolerances

3D Scan-Based Reverse Engineering of Differential Bevel Gears

Sylvain Mayoux and Denis Barday

Inter-wheel differentials utilizing straight bevel gears are commonly used in the automotive industry to accommodate the relative speed differences between wheels during cornering. These mechanical systems have been integral to vehicle design for over a century, often carried over from one project to another. Consequently, the expertise and knowledge surrounding these systems can sometimes be lost, leading to challenges in design continuity and innovation. This gap in knowledge underscores the necessity for developing effective reverse engineering methods for differential gears. Such methods are essential not only for recovering lost design information but also for conducting comprehensive analyses of competitor products. The advent of advanced 3D scanning technology has revolutionized the field, providing new opportunities for the efficient and accessible reverse engineering of complex components. This study aims to propose a robust reverse engineering methodology for straight bevel gears, especially for those found in inter-wheel differentials. By leveraging 3D scans of sun and planet gears, an innovative approach to accurately reconstruct the macrogeometry parameters of these critical mechanical systems is proposed. The rebuilt geometry was used to create a measurement grid for flank topography evaluation. These measurements were used to extract the contact ease-off, thereby revealing the complete macro and microgeometry of the previously unknown differential gears.

3D Scanning

The method described in this paper is specifically illustrated through the analysis of a planet gear from a commercial vehicle inter-wheel differential. It is assumed that the original geometrical parameters of this design are unavailable and required for further studies. The process begins with 3D scanning of both the sun and planet gears. The planet gear was scanned twice: first while supported on its back face as shown in Figure 1 (left) and then inverted upside down. Each scan generated approximately 30 million data points. These scans were subsequently merged and exported in STP format, resulting in a refined dataset containing over 40,000 points. The Cartesian coordinates of each node defining the 3D shape of the part were then extracted, as shown in Figure 1 (right).

Basic Parameters

In parallel with the first step, the tooth count of the sun and planet gears, along with their respective mounting distances, can be determined through basic measurement and evaluation. All gear-related terms and symbols used in the following sections comply with ISO 1122-1 (Ref.1). The tooth count of both members is essential for determining the pitch angle, which is defined by Equation 1.

$$\delta_1 = a\tan\left(\frac{z_1}{z_2}\right) \qquad (1)$$

Where:

δ_1 is the planet gear pitch angle
z_1 is the number of teeth of the planet gear
z_2 is the number of teeth of the sun gear

The mounting distances of the planet gears t_{B1} can be obtained from the differential housing by measuring the distance between the contact surfaces of two opposite planet gears using a caliper. If a friction washer is present between the

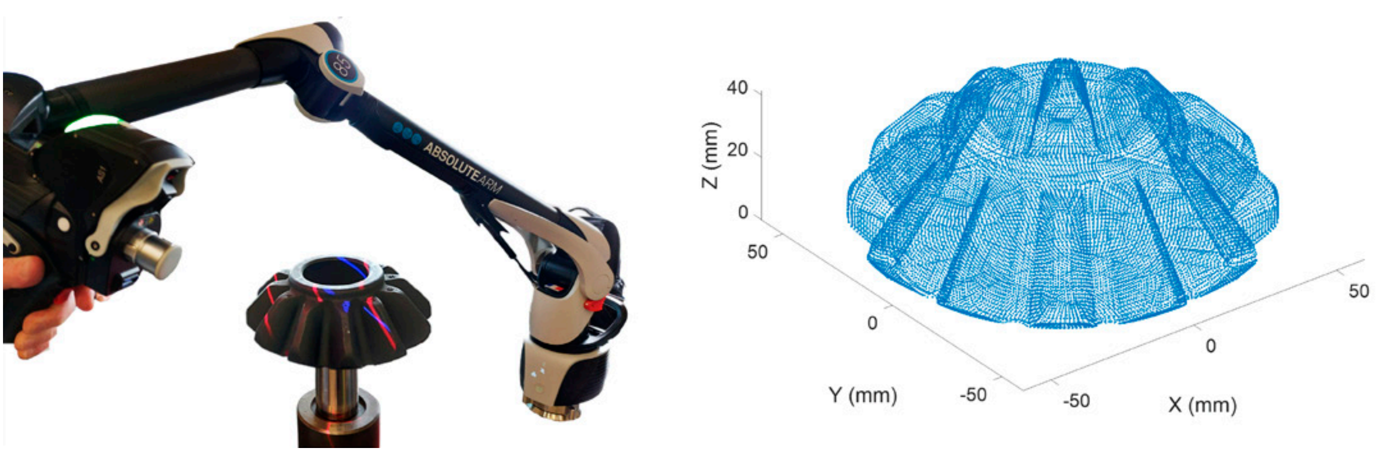

Figure 1—3D scanning of planet gear (left) and point extract (right).

planet gear's back face and the differential nest, its thickness should be included when estimating the mounting distance, as illustrated in Figure 2.

RZ Projection

Once the basic geometry has been established, the Cartesian coordinates obtained from 3D scanning are projected onto the RZ plane. The objective of this step is to determine the face angle (δ_{a1}) and root angle (δ_{f1}) along with the face apex beyond crossing point (t_{zF1}) and root apex beyond crossing point (t_{zR1}) of the scanned planet gear.

For that purpose, the highest and lowest points along the gear flank—defining the face and root cones, respectively—were identified and isolated. These sets of points should form straight, continuous lines. Any points associated with root reinforcement shapes, blank outer radius, or chamfers were visually identified and removed from their respective sets. In Figure 3, root points are highlighted in blue, while face points are marked in red. A linear equation was fitted through both sets of points. For the face points, an equation in the form

$$Z = a_{a1} * R + b_{a1} \tag{2}$$

was obtained. From this equation, the face angle (δ_{a1}) and face apex beyond crossing point (t_{zF1}) can be determined using Equations 3 and 4:

$$\delta_{a1} = a\tan\left(-\frac{1}{a_{a1}}\right) \tag{3}$$

$$t_{zF1} = b_{a1} - t_{B1} \tag{4}$$

A negative value indicates that $t_{zF1}<t_{B1}$, as illustrated in Figure 3. A similar process is applied to the root points to estimate the root angle (δ_{f1}) and root apex beyond crossing point (t_{zR1}).

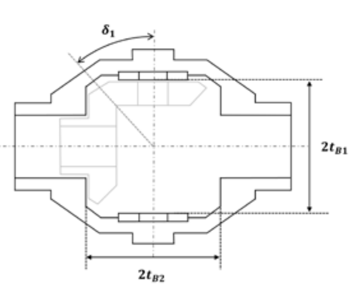

Figure 2—Differential housing and mounting distances.

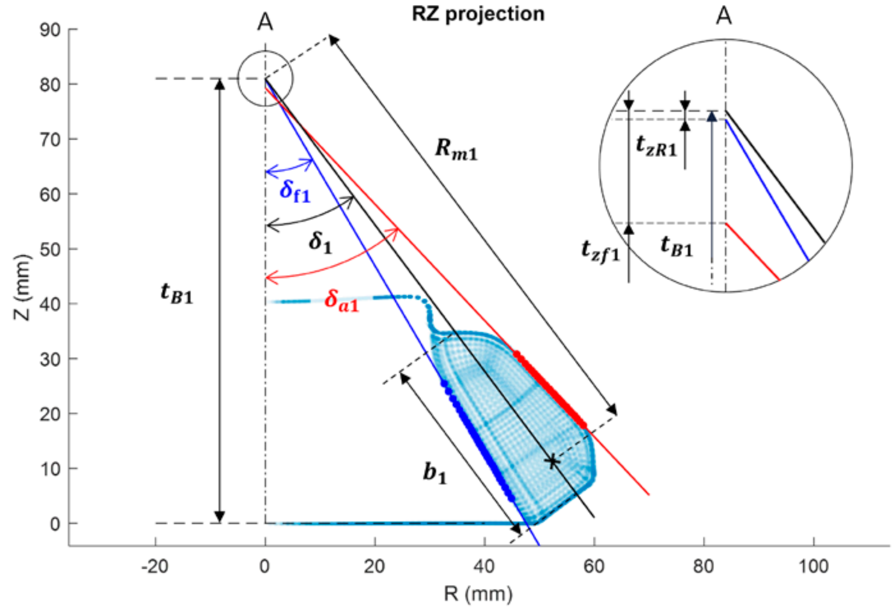

Figure 3—RZ projection of planet gear points.

At this stage, the pitch angle δ_1 previously defined can also be plotted on the RZ graph, given that the pitch line intersects the crossing point of RZ coordinates (0, t_{B1}). The pinion face width (b_1) was estimated as the absolute distance between the first and last point of the projected profile that intersects the pitch line.

Finally, a cone distance (R_{m1}) was arbitrarily defined by selecting a point along the pitch line and within the limits of the previously defined face width. This reference point will be used in the next steps to establish a transverse section of the gear. Within this section, the meshing of a straight bevel gear is considered equivalent to the meshing of a cylindrical spur gear with virtual geometric parameters. This transverse section will be used to estimate the tooth thickness, pressure angle and tool tip radius.

Transverse Section and Tooth Thickness

From the 3D-scanned dataset, a single tooth was isolated. A plane perpendicular to the pitch line, passing through the cone distance R_{m1} was defined and designated as plane A-A in XZ and YZ projections, as shown in Figure 4 (left). The points whose distance from the plane was less than a predefined limit were identified and projected onto the latter. Simultaneously, the pitch points (P) on the left and right flanks were identified as the intersection of the transverse section points with the pitch line, illustrated with a dotted line in Figure 4 (top left). These points were then shifted in the x direction to ensure that both pitch points were equidistant from the y-axis. It can be noted that the distribution of the transverse section points closely resembles that of a cylindrical spur gear with an involute profile, exhibiting the following characteristics:

$$m_{et} = \frac{2 * R_{m1} * \sin(\delta_1)}{z_1} \tag{5}$$

$$d_{e1} = 2 * R_{m1} * \tan(\delta_1) \tag{6}$$

$$z_1' = \frac{z_1}{\cos(\delta_1)} = \frac{d_{e1}}{m_{et}} \tag{7}$$

Where:

m_{et} is the transverse module

z'_1 is the virtual number of teeth of the pinion

d_{e1} is the pitch diameter of the virtual cylindrical gear

Since this pitch diameter should intersect the two previously identified pitch points, the transverse section points were shifted in the y direction so that these points align with d_{e1}. From this, the tooth thickness half-angle (ψ_1) was calculated based on the adjusted pitch point coordinates. Finally, the mean normal circular tooth thickness (s_{mn1}) was determined using:

$$s_{mn1} = d_{e1} * \psi_1 \tag{8}$$

Transverse Section and Pressure Angle

The normal pressure angle (α_n) of the virtual cylindrical involute gear is defined as the angle formed between a radial line of the pitch circle and the tangent line to the profile at the pitch point (Ref. 2). It can be estimated from the transverse section by following the steps illustrated in Figure 5 and described below.

- Step 1: A circle centered at the previously identified pitch point (P) on one of the flanks was defined, with a search radius (r_s). The points of the transverse section located within this circle were identified.
- Step 2: A circle was fitted through the identified set of points to estimate the local profile radius of curvature at the pitch point. The coordinates of the center of this fitted circle, denoted as X_C, were retrieved.
- Step 3: A line passing through the pitch point and the fitted circle center X_C was drawn, establishing the normal to the gear surface. The perpendicular to this normal, also passing through the pitch point, provides the tangent line to the profile at the pitch point.
- Step 4: A radial line of the pitch circle was defined as passing through the center of the gear O_C (0,0) and the pitch point.
- Step 5: The normal pressure angle (α_n) was estimated by calculating the angle between the tangent line (from Step 3) and the radial line (from Step 4).

It should be noted that these results may vary depending on the initial choice made for the search radius (r_s). In this study, consistent and repeatable results were obtained with r_s ranging from 15–25 percent of the tooth height.

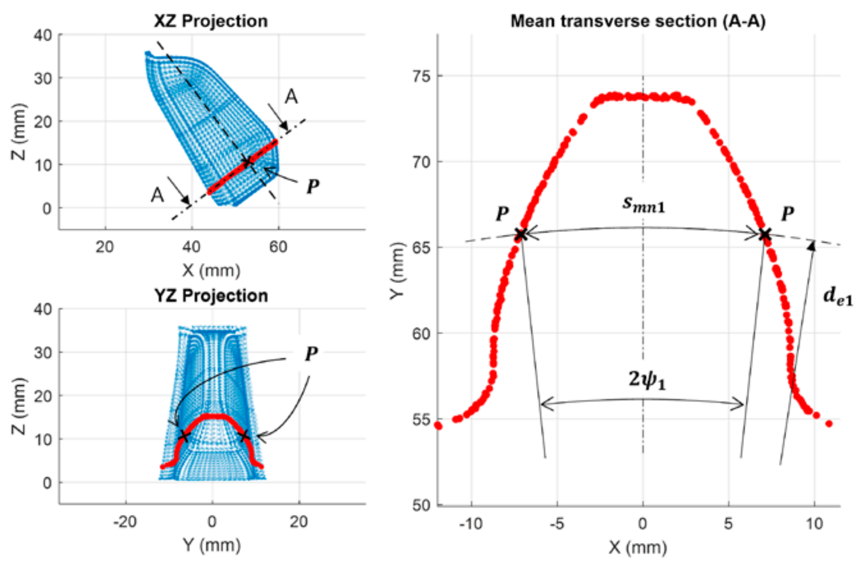

Figure 4—Transverse section and pitch point alignment.

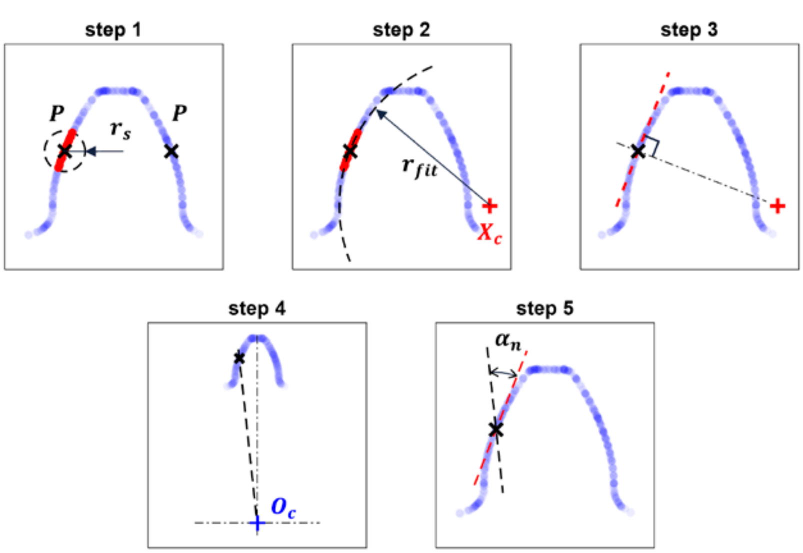

Figure 5—Estimation of normal pressure angle.

Profile Shift, Addendum and Dedendum Calculation

Once the mean normal circular tooth thickness (s_{mn1}) and normal pressure angle (α_n) have been determined, the profile shift coefficient (x_{hm1}) can be obtained using the following equation:

$$s_{mn1} = 0.5 * m_{et} * \pi + 2 * m_{et} * x_{hm1} * \tan(\alpha_n) \quad (9)$$

The addendum coefficient (h_{ae1}) and dedendum coefficient (h_{fe1}) of the straight bevel planet gear at the cone distance R_{m1} be determined using the face angle (δ_{a1}), root angle (δ_{f1}), face apex beyond crossing point (t_{zF1}) and root apex beyond crossing point (t_{zR1}) as defined in the previous section "RZ Projection":

$$t_{zR1} = -h_{fe1} * \sin(\delta_1) + 0.5 * \frac{d_{fe1}}{\tan(\delta_{f1})} - R_{m1} * \cos(\delta_1) \quad (10)$$

$$t_{zF1} = h_{ae1} * \sin(\delta_1) + 0.5 * \frac{d_{ae1}}{\tan(\delta_{a1})} - R_{m1} * \cos(\delta_1) \quad (11)$$

Where
d_{fe1} is the root diameter of the planet gear
d_{ae1} is the tip diameter of the planet gear

These diameters are derived from the equivalent spur gear tip diameter (d'_{a1}) and root diameter (d'_{f1}) as follows:

$$d_{fe1} = d'_{f1} * \cos(\delta_1) \quad (12)$$

$$d_{ae1} = d'_{a1} * \cos(\delta_1) \quad (13)$$

The equivalent spur gear diameters are given by:

$$d'_1 = m_{et} * z'_1 \quad (14)$$

$$d'_{f1} = d'_1 + 2 * (x_{hm1} - h'_{f1}) * m_{et} \quad (15)$$

$$d'_{a1} = d'_1 + 2 * (x_{hm1} - h'_{a1}) * m_{et} \quad (16)$$

Where:
h'_{a1} is the addendum coefficient of the equivalent spur gear
h'_{f1} is the dedendum coefficient of the equivalent spur gear

These coefficients can be expressed in terms of profile shift coefficient (x_{hm1}):

$$h'_{a1} = \frac{h_{ae1}}{m_{et}} - x_{hm1} \quad (17)$$

$$h'_{f1} = \frac{h_{fe1}}{m_{et}} + x_{hm1} \quad (18)$$

By substituting Equations 17 and 18 back into Equations 10 and 11, the values of h_{ae1} and h_{fe1} can be isolated and calculated.

Transverse Section and Tool Tip Radius

The edge radius of the hobbing tool (r_{a0}) has been shown to be proportional to the minimum radius of curvature (ρ_f) in the generated root fillet (Ref. 3). This minimum radius occurs at the beginning of the trochoid, at a point where the profile is tangent to the root diameter. At this point, the relationship between these parameters is expressed as follows:

$$\rho_f = r_{a0} + \frac{(h'_{f1} - r_{a0})^2}{0.5d_{e1} + (h'_{f1} - r_{a0})} \quad (19)$$

Since the pitch diameter (d_{e1}) and dedendum coefficient of equivalent spur gear (h'_{f1}) were determined in the section "Profile Shift, Addendum and Dedendum Calculation," the only unknown in this equation required to determine r_{a0} is the radius of curvature (ρ_f). To determine the latest, the transverse section previously established was analyzed. The points of the root fillet close to the root diameter were isolated (highlighted in red in Figure 6). A circle was then fitted through these points, allowing for an estimation of ρ_f as illustrated in Figure 6.

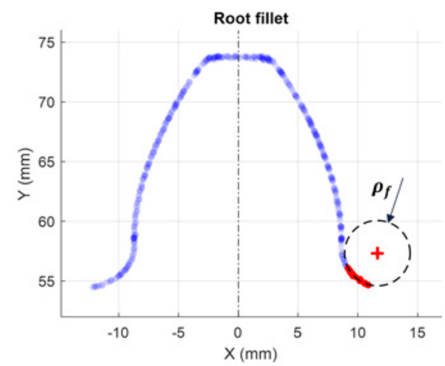

Figure 6—Estimation of the radius of curvature (ρ_f) in the generated root fillet.

The edge radius of the hobbing tool (r_{a0}) was isolated from Equation 19. To reduce the uncertainty of the proposed method, this operation was repeated for the left root fillet. The mean of both obtained values was considered as the final value for r_{a0}.

Numerical Data and Overall Check

Table 1 below presents the measured results obtained from the planet gear analyzed in this study, following the methodology described in previous sections. For confidentiality reasons, only the pinion data are provided in this article. However, the analysis was thoroughly conducted on both the sun and planet gears.

Using the measured data from Table 1, the remaining geometrical parameters were computed using the equations provided in this study. Results are provided in Table 2.

A simple approach to validate the identified macrogeometry is to compute, in a transverse section defined by its cone distance R_m all the geometrical

Description	Symbol	Unit	Value
Number of teeth (pinion)	z_1	-	12
Number of teeth (gear)	z_2	-	16
Mounting distance	t_{B1}	mm	81
Cone distance	R_{m1}	mm	88
Face width	b_1	mm	27.8
face angle	δ_{a1}	°	43.34
root angle	δ_{f1}	°	30.46
face apex beyond crossing point	t_{zF1}	mm	-2.08
root apex beyond crossing point	t_{zR1}	mm	-0.14
Tooth thickness half angle	ψ_1	°	6.21
Normal pressure angle	α_n	°	27.0
Minimum radius of curvature at root fillet	ρ_f	mm	2.48

Table 1—Measured numerical data from physical parts using the proposed methodology.

Description	Symbol	Unit	Value
Pitch angle	δ_1	°	36.87
Equivalent pitch diameter	d_{e1}	mm	105.6
Mean normal circular tooth thickness	s_{mn1}	mm	14.32
Transverse module	m_{et}	mm	8.8
Virtual number of teeth of equivalent spur gear	z'_1	-	15
Profile shift coefficient	x_{hm1}	-	0.055
Addendum coefficient	h_{ae1}	-	8.543
Dedendum coefficient	h_{fe1}	-	9.958
Edge radius of the tool	r_{a0}	mm	1.232

Table 2—Numerical data calculated using provided equations.

parameters of the equivalent cylindrical spur gear. From there, using equations for involute profile and trochoidal root, one can compare the theoretical tooth shape with the physical points of the scanned dataset at the defined section. This comparison is illustrated in Figure 7, where the theoretical tooth shape is represented as a dark continuous line, while the physical scanned points appear as blue scattered points. The comparison is performed at two different cone distances—close to the toe and heel of the planet gear—both different from the one at which the analysis was conducted.

At this stage, the complete macrogeometry of the differential has been identified. These data are sufficient to establish a complete gear datasheet and run basic strength calculations, including surface durability and tooth root strength as per ISO 10300 (Ref. 4). However, an additional step could be achieved by overcoming the challenge of accurately reconstructing the microgeometry of both gears.

Topographic Measurement and Contact Ease-Off

In this final section, the gear blank shape was extracted from an RZ projection, capturing parameters such as the back cone angle, root reinforcement and tip radii, as shown in Figure 8 (left). Using this data alongside the previously determined macrogeometry, an initial approximation of the tooth surface microgeometry was established.

To refine this approximation, a 15 x 15 measurement grid was created, precisely following the gear contour, as depicted in Figure 8 (right). Each grid point contains x,y,z coordinates and the normal to the tooth surface.

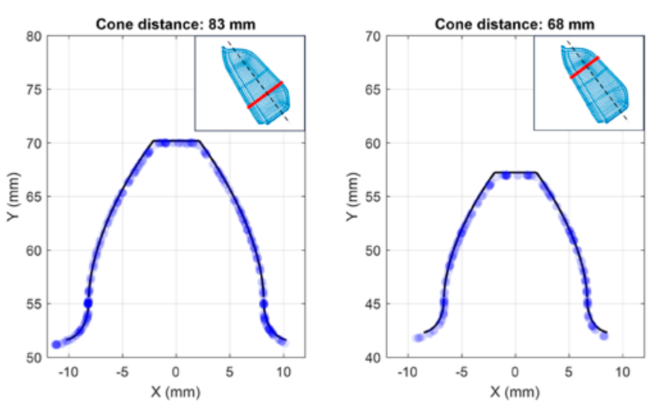

Figure 7—Theoretical tooth shape vs. transverse section points.

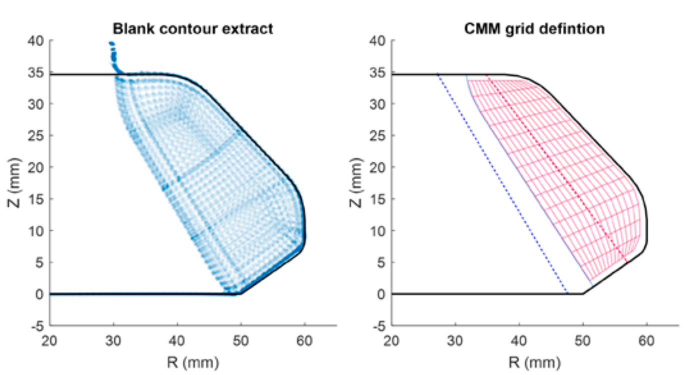

Figure 8—Blank contour extract, CMM grid and contact ease-off.

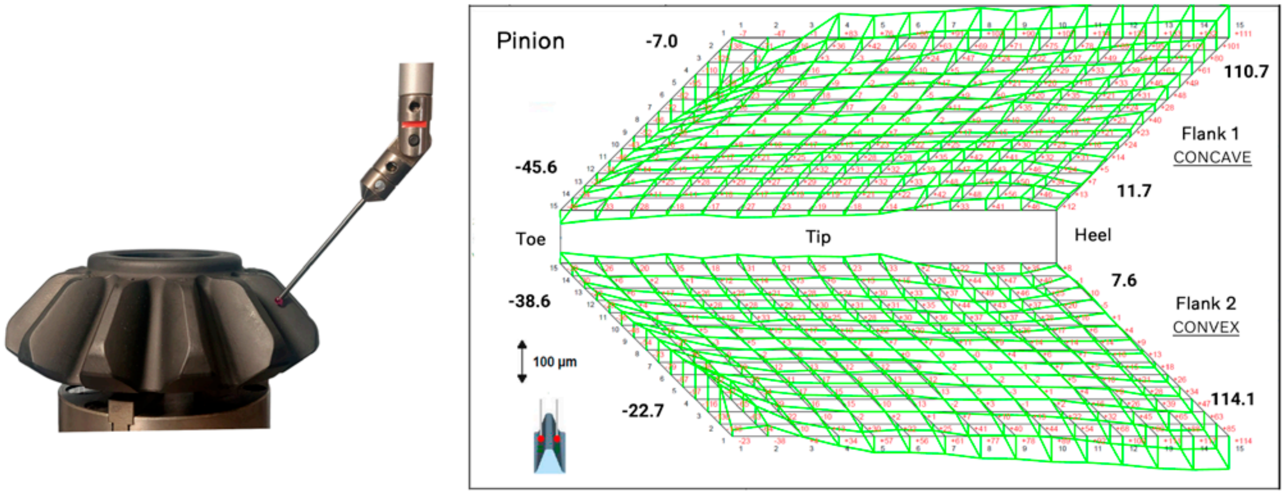

Figure 9—CMM evaluation and inspection report.

The planet gear analyzed in this study was then placed on a coordinate measuring machine (CMM) to measure the exact surface deviation at each point in the normal direction, as presented in Figure 9 (left). The CMM inspection report (Figure 9, right) revealed reasonable amplitudes of the surface deviation, confirming the validity of the initial microgeometry assumption. The final microgeometry was determined by combining the initial estimation with the measured deviations.

Applying the same method to the side gear enables the determination of the geometric ease-off. The extracted ease-off topography is represented on the pinion in Figure 10 (left) as the initial gap (in µm) between mating gears. From this, standard finite element (FE)-based bevel gear calculation can be performed, enabling the accurate evaluation of durability under load, contact patterns, transmission errors and overall performance. An example is provided in Figure 10 (right), illustrating the simulated no-load contact pattern on the planet gear.

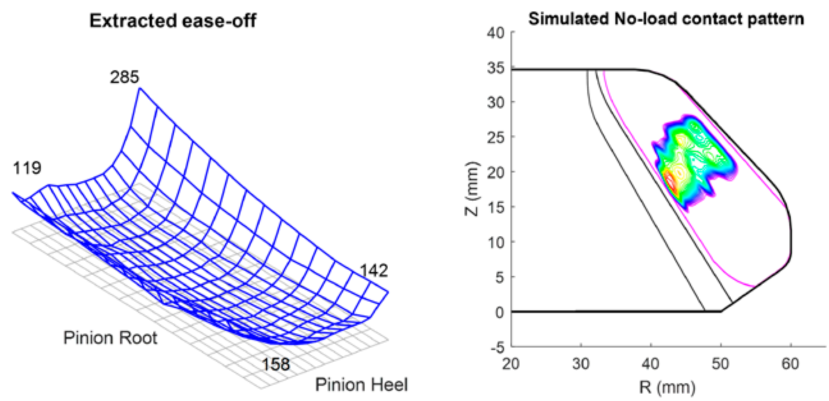

Figure 10—Extracted ease-off (gap in µm) and simulated no-load contact pattern.

Conclusion

This study presented a structured methodology for reverse-engineering the macro and microgeometry of a straight bevel gear, relying on 3D scanning, mathematical modelling and topographic measurement. Through a step-by-step approach, key geometrical parameters—including tooth thickness, pressure angle, profile shift and tool tip radius—were identified and validated against physical measurements. The final step relied on CMM for topographic evaluation to identify the microgeometry and assess contact ease-off, enabling further numerical simulations for performance evaluation. The extracted data can serve as a foundation for durability assessments and design optimization, contributing to the accurate evaluation and enhancement of gear performance.

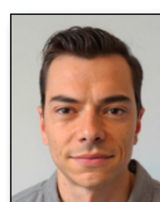

Sylvain Mayoux studied Mechanical Engineering at INSA de Lyon. He has been working for the Volvo Group since 2018 in the field of gear design and simulation.

Denis Barday is the Volvo Group expert for bevel gears. He has been working in gear design for over 30 years, developing FE-based calculation tools for cylindrical and bevel gears.

References

1. International Organization for Standardization (ISO). (1998). ISO 1122-1: Vocabulary of gear terms—Part 1: Definitions related to geometry.
2. American Gear Manufacturers Association (AGMA). (2005). Gear nomenclature: Definition of terms with symbols (ANSI/AGMA 1012-G05). ISBN 1-55589-846-7. OCLC 65562739.
3. Townsend, D. P. (1992). *Dudley's Gear Handbook.* McGraw-Hill, New York.
4. International Organization for Standardization (ISO). (2014). ISO 10300: Calculation of load capacity of bevel gears—Parts 1–3. Second edition, April 1, 2014.

Nanocomposite Coatings for Gears

Dr. Peter L. Schmidt, P.E. and Brady Blomquist

Introduction

Small reductions in friction can result in large savings in power requirements, particularly at high speed. Lowering the viscosity of lubricating oils helps, but there is a lower limit on lubricant viscosity where functionality in the application is retained. Nanocomposite thin-film coatings have been employed in various applications to reduce sliding friction and surface wear and are proposed for use in gear applications.

This work aims to demonstrate the potential benefit of applying nanocomposite coatings to gear teeth to reduce operating friction and wear by presenting tribological test data.

A brief history of thin film coating technology development history is given in the following paragraphs (Refs. 1, 2).

World War II Era

Optical Coatings: During World War II, the demand for improved optics led to advancements in optical coatings. Antireflective coatings, composed of thin films, were developed to enhance the performance of lenses and other optical devices.

Post-World War II

Thin-Film Deposition Techniques: In the post-war period, there was significant progress made in thin-film deposition techniques. Vacuum deposition methods emerged, such as Physical Vapor Deposition (PVD) and Chemical Vapor Deposition (CVD). These techniques enabled precise control over coating thickness, microstructure, and composition, laying the foundation for developing nanocomposite coatings.

1950s–1960s

Semiconductor Industry: The semiconductor industry's growth in the 1950s and 1960s drove advancements in thin-film technology. Thin films became integral to the manufacturing of semiconductors, with techniques like sputtering and evaporation becoming widely adopted.

1970s–1980s

Plasma-Assisted Techniques: The use of plasmas to assist in thin-film deposition gained prominence in the 1970s and 1980s. Plasma-Assisted Chemical Vapor Deposition (PACVD) and Plasma Enhanced Chemical Vapor Deposition (PECVD) techniques were developed, improving thin film coatings' mechanical and chemical properties and lowering processing temperatures.

Late 20th Century

Advancements in Coating Materials: Continued research led to the development of a wide range of coating materials. Thin films were now being applied not only for functional purposes like corrosion resistance and optical enhancement but also for novel applications in electronics, sensors, and medical devices.

Nanocomposite Coatings

Nanotechnology and Multifunctional Coatings: The 21st century has seen a convergence of nanotechnology and thin-film coatings. Nanocomposite coatings, with nanoscale materials embedded, have become a focus for enhanced properties. Multifunctional coatings have gained significant attention, offering a combination of properties such as self-cleaning, anti-bacterial, and enhanced mechanical properties.

United Protective Technologies, LLC (Ref. 3), has expanded the technology of thin film coatings by using custom-engineered reactors, along with low-temperature application strategies, to produce coatings that reduce friction. These coatings often reduce friction by more than 50 percent and increase wear resistance by orders of magnitude. The low process temperature used to apply these coatings means that the heat treatment done to most gears before placing them in service is not affected by this application process, allowing it to be the final production step before placing a component in service.

Figure 1 shows the basic structure of a nanocomposite coating. The image displayed shows the layered coating, adhesion layer, and substrate, revealed by the process described in ISO 26423 (Ref. 4). A 15 mm diameter steel ball, using diamond paste as an abrasive, is used to grind through the coating to expose a section used to make a thickness measurement. Different coating systems have different layers and can have different layer mechanical properties and chemical compositions.

Specific Coating System Parameters

The coating system studied in this work, United Protective Technologies P51M, is a nanocomposite coating system comprised of a metallic adhesion layer and multiple nanocomposite functional layers. Its applied thickness is 3–5 microns.

A version of this paper was first presented at the 2024 Fall Technical Meeting (FTM), October 7–9, 2024, Rosemont, IL. Printed with permission of the author(s). Statements presented in this paper are those of the author(s) and may not represent the position or opinion of the American Gear Manufacturers Association.

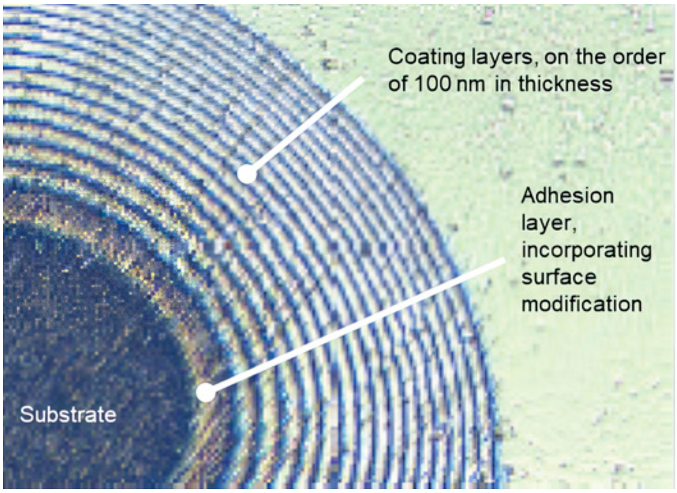

Figure 1—Image of the features of a nanocomposite coating after performing the ISO 26423 coating thickness measurement procedure

Figure 2—Air Force T-38 Talon, in flight (Ref. 6).

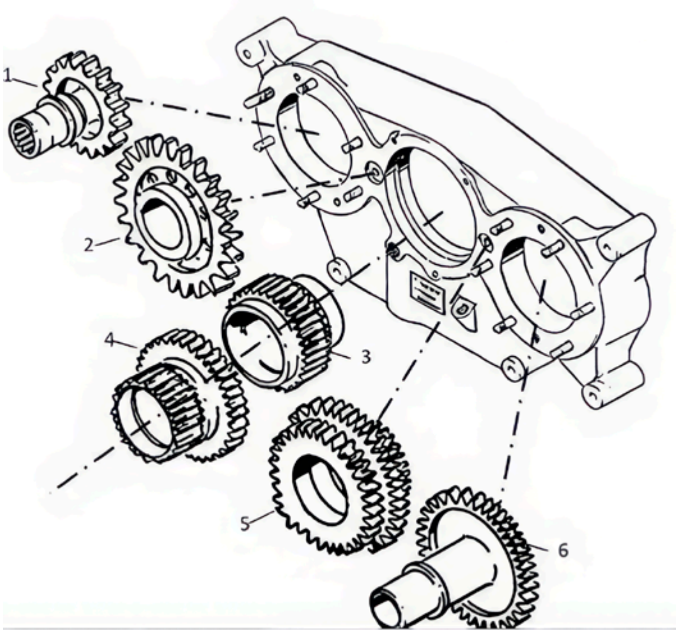

Figure 3—Project gearbox exploded view.

Application

This work was funded as an SBIR project (Ref. 5) entitled "Super Lubricity Interface Coatings (SLIC)", under topic AF203-DCS01, and was formulated to study and improve the performance of aerospace service gears used in the J85 turbine engine deployed on T-38 aircraft, shown in Figure 2, in service with the US Air Force. The current coatings used on many high friction aircraft components are outdated, and due to the low temperature final stage deposition of the UPT coating item configuration can remain the same, allowing the Air Force an economically viable method of improving the properties of these key components. The T-38 aircraft continues to be the quintessential training jet in the Air Force fleet, however, with the T-7 Redhawk positioned to take its place the need to develop economically viable improvements are of key importance for keeping the aging fleet performing in the interim.

System Description

The gears are part of a gearbox assembly designed by Northrop NORAIR division in 1961, which pulls power from the main turbine shaft to drive hydraulics and provide electrical power to aircraft systems in flight. Due to the hydraulic pump and electrical generator needs, the gearbox utilizes an oil-based hydraulic/centrifugal mechanism to shift between a disk clutch and a sprag clutch for low-speed and high-speed conditions, respectively. Most gearboxes are produced through the repair and overhaul procedure, refurbishing and reusing key components, including all gears where possible.

Hardware Description

The gears are arranged in series, as shown in Figure 3, except for gears 3 and 4. The input shaft, being the central shaft for both Gears 3 and 4, transmits power from the engine to the rest of the gearbox through either Gear 3 or Gear 4, via the sprag clutch or the disk clutch, respectively, depending on the input speed. All are spur gears, with two gears being of compound configuration. The gears are manufactured from AISI 4620 or AISI 8620 steel, with AISI 8620 being preferred due to market demand and availability limitations. All testing for this project was performed with specimens manufactured from AISI 8620 steel, which was carburized and heat-treated per the gear drawings.

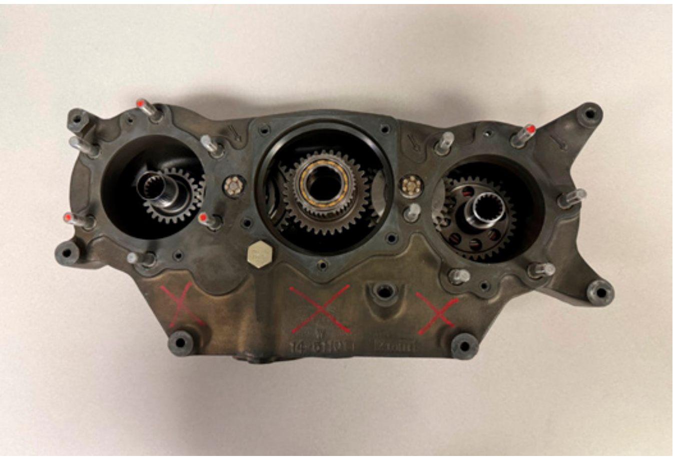

Figure 4—Project gearbox assembly.

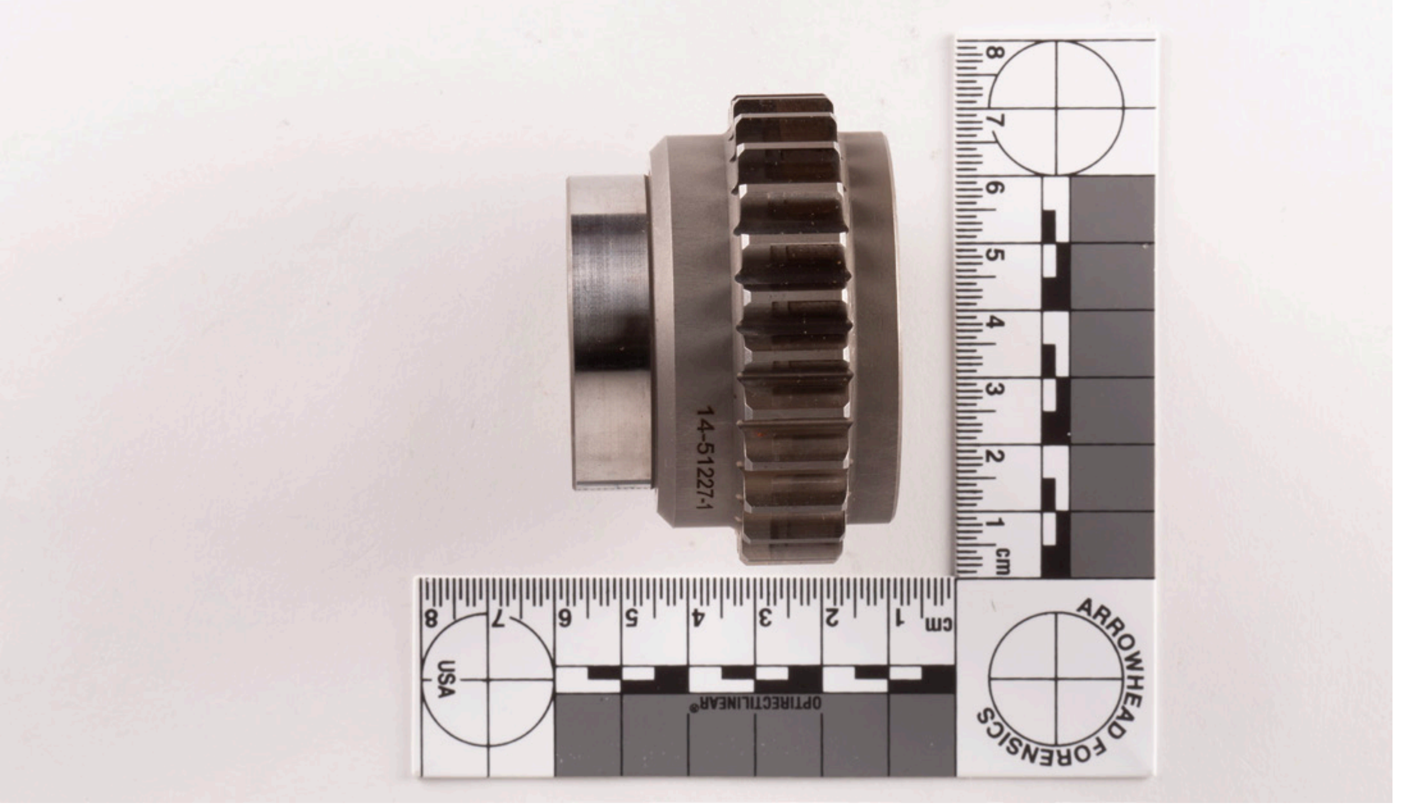

Figure 5—Sprag Clutch Gear (Gear #3) with scale for reference.

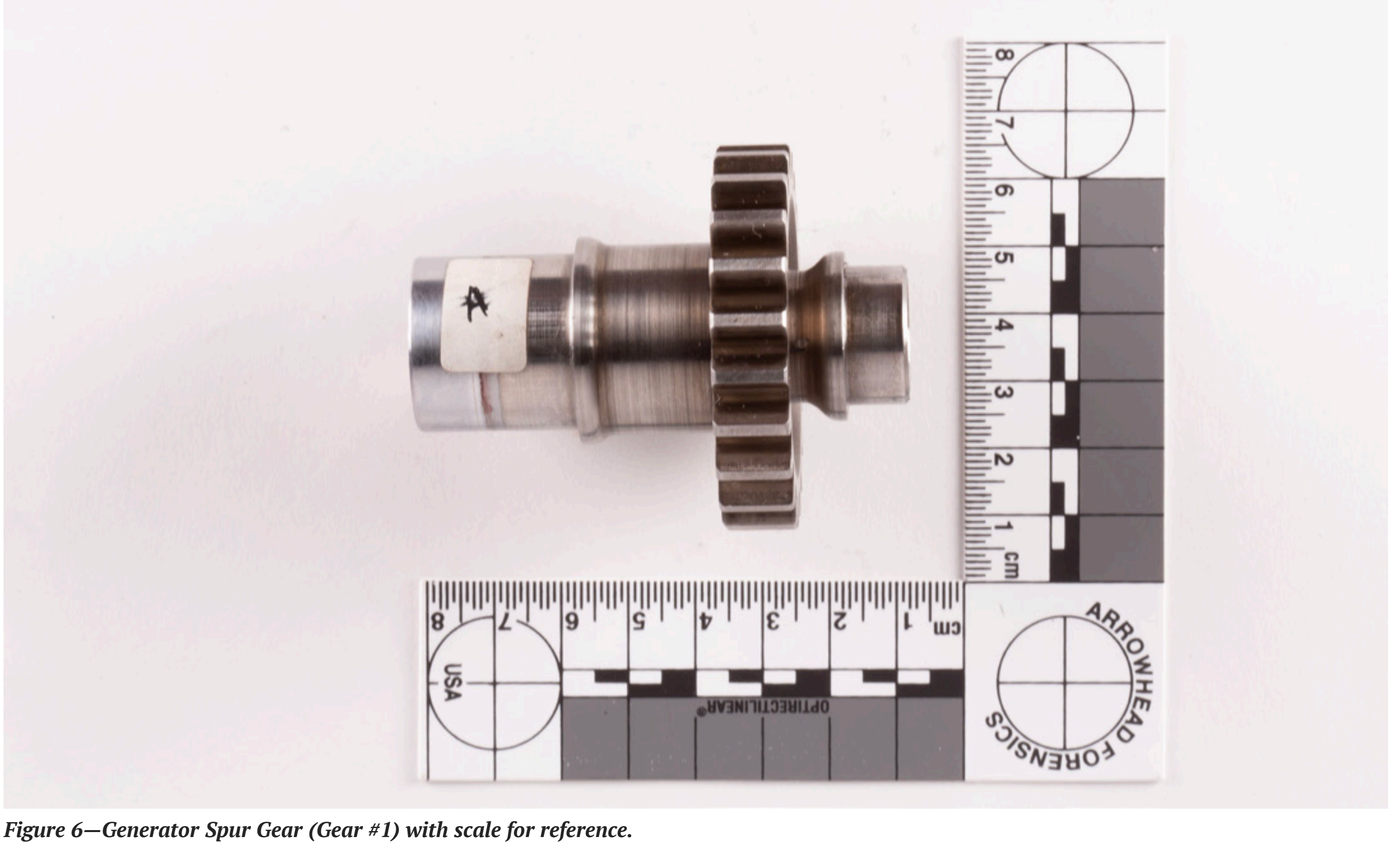

Figure 6—Generator Spur Gear (Gear #1) with scale for reference.

Figures 5-6 show selected gears, with scales for reference.

Figures 7-8 show the typical wear and damage seen on gears recovered during overhaul operations.

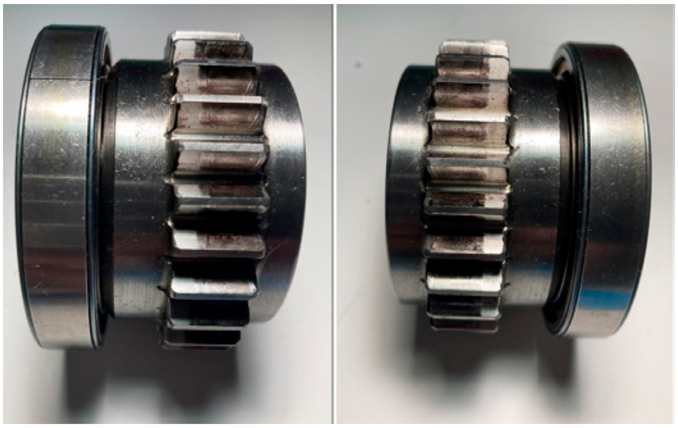

Figure 7—Sprag Clutch Gear (Gear #3) pictured with its support bearing in place.

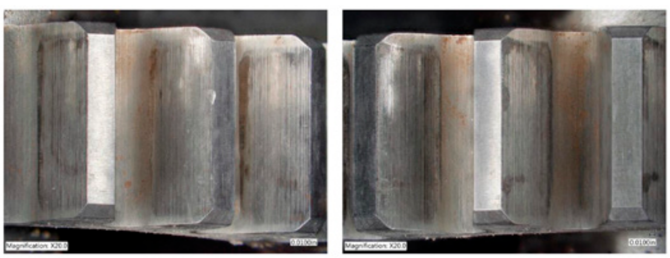

Figure 8—Generator Spur Gear (Gear #3) showing typical wear seen at overhaul.

Table 1 shows the gear connectivity.

Gear #	Nomenclature
1	Generator Spur Gear
2	Spur Idler Gear
3	Sprag Clutch Gear
4	Disk Clutch Gear
5A	Cluster Gear
5B	Cluster Gear
5C	Cluster Gear
6	Hydraulic Pump Gear

Table 1—Gear nomenclature.

Gear 5 is a compound gear with three different diameters. The three gear profiles can be seen on the drawing as A, B, and C. Track A has the smallest pitch diameter, Track B has the largest pitch diameter, and Track C has the intermediate pitch diameter. That naming convention has been preserved in this document.

Operating Parameters

The gears are lubricated with MIL-PRF-7808 turbine engine lubricating oil and run in a semi-submerged bath. This fluid is filtered and cooled such that the maximum operating temperature never exceeds 250°F. Contact stress was calculated as a first step in the analysis.

The AGMA equation used was of the form (Ref. 7):

$$S_c = C_p\left[W_t K_v K_o K_s \frac{K_m}{Fd}\frac{C_f}{I}\right]^{\frac{1}{2}} \quad (1)$$

Where C_p is an elastic matching parameter given by:

$$C_p = \left[\frac{1}{\pi\left(\frac{1-\mu_P^2}{E_P}+\frac{1-\mu_G^2}{E_G}\right)}\right]^{\frac{1}{2}} \quad (2)$$

Where W_t is the transmitted force, K_v is a stress concentration factor for the velocity of operation, K_o is a stress concentration factor for loading type, K_s is a stress concentration factor for gear tooth size, K_m is a stress concentration factor for load distribution across the flank of the gear, C_f is a stress concentration factor for surface finish of the gear, F is the minimum width or flank of the gear tooth in the mesh pair, d is the pitch diameter of the pinion of the two gears in mesh (the gear with the smallest pitch diameter), and I is a geometry correction factor for the involute gear tooth shape, which for an external spur gear is given by Ref. 8:

$$I = \frac{\cos\phi \sin\phi_t}{2m_N}\frac{m_G}{m_G+1} \quad (3)$$

Gear contact stress calculations for each gear pair at both input speeds assumed the following:

1. The 2,200 in-lb$_f$ input torque represented a transient load on the gear train. An overload factor of K_O = 2.25 was applied to account for this loading profile.
2. All gears were carburized and heat-treated to a case hardness of 58–60 on the Rockwell C scale.
3. The factor modifying the bearing stress calculations based on potential misalignment (K_m) was 1.03, assuming well-centered and well-supported gears.
4. Gear surface speed was calculated for each gear and used to generate factors in the equations as dictated by AGMA.
5. The geometry stress concentration factor was calculated using the gear pressure angle of 20 degrees, with individual gear pairs having discrete values for this factor.
6. The elastic matching factor assumed all gears were manufactured from AISI 4620/8620 steel.
7. The surface roughness factor (C_f) assumed all gear teeth in mesh had surface finishes of 32 microinch rms, yielding a roughness factor of 1.1.
8. Stresses were calculated based on the minimum gear flank in the mesh and the pitch diameter of the pinion of the two gears in the mesh.

The following results were obtained using the equation shown based on these assumptions. These results represent the maximum stresses present on gear flanks based on the shock load provided. All the results for contact stresses can be seen in the two tables below, one for each speed of operation supplied.

Gear #	Pinion #	Contact Stress (lb_f/in^2)	Contact Stress (MPa)
2	3	400.561E+3	2.762E+3
2	1	416.367E+3	2.871E+3
5B	3	434.178E+3	2.994E+3
6	5A	516.683E+3	3.563E+3

Table 2—Estimated maximum stress at high-speed operation.

Gear #	Pinion #	Contact Stress (lb_f/in^2)	Contact Stress (MPa)
2	3	393.689E+3	2.715E+3
2	1	410.460E+3	2.831E+3
4	5C	406.964E+3	2.807E+3
6	5A	511.135E+3	3.525E+3

Table 3—Estimated maximum stress at low-speed operation.

These results can be compared to the allowable bearing stress. The material constant is modified according to the following relationship:

$$s_c = \frac{s_{ac}}{S_H}\frac{Z_N C_H}{K_T K_R} \tag{4}$$

where s_{ac} is the gear material's constant allowable bearing stress, C_H is a hardness ratio factor, K_T is a stress concentration factor based on service temperature, and K_R is a stress concentration factor based on desired reliability. S_H is a safety factor.

We consider the following for values in this relationship:

1. The AGMA standard identifies the maximum bearing stress allowable for carburized, hardened steel gears as 275 x 10^3 psi (Grade 3 steel gears).
2. We assume that Y_N takes a value of unity, i.e., that the gears were designed for a life of 10^6 cycles, which is the standard approach.
3. For this analysis, we assume a safety factor of unity.
4. K_T also takes a value of unity since the service temperature is less than or equal to 250°F.
5. K_R takes a value of 0.68, as shown next.

The life expectancy of the gears in this device was 2,500 hours MTBF, with a replacement time of 2,250 hours. This can be converted to reliability (in percent) using the following Ref. 9:

$$R(t) = exp\left(\frac{-t}{MTBF}\right) \tag{5}$$

This yields a reliability of 41 percent. The minimum reliability considered by AGMA is 50 percent, which produces a value for K_R using:

$$K_R = 0.658 - 0.0759 * ln(1 - R(t)) = 0.68 \tag{6}$$

This value is a bit more conservative than the value shown in Table 11 of Ref. 7. Using this stress concentration factor, our allowable stress for the gears under analysis would be 404 ksi. This calculated allowable stress value seems to be exceeded in six use cases. All the loads and contact stresses during in-house tribology tests were decided based on these calculations. According to the analysis, these gears exceeded the allowable contact stresses in six studied cases, as seen in Tables 2 and 3.

Testing Rationale

The failures reported for the gears under study indicate that there is surface interaction attributable to high friction and excessive sliding wear of meshing surfaces due to adhesion or localized failure of the gear material. The high stress present in the gear mesh suggested to the investigation team that a nanocomposite coating could benefit the system. A nanocomposite coating assists with wear and frictional performance. This may reduce interfacial temperature, leading to improved substrate and lubrication durability. Testing was undertaken to demonstrate the improved lubricity that the nanocomposite coating offers and its ability to improve wear resistance.

Coating Performance Testing

Standard tribological testing was performed on the coating as a gate for further, more extensive testing. Upon completion of tribological testing, two types of scuffing tests were undertaken to demonstrate the potential benefits to gear performance attainable by applying the coating under study.

Effect on Substrate Material Properties

Since this coating has not been widely applied to gears and has never been deployed on aerospace platforms, the project sponsor requested that coated parts be subjected to material property tests normally associated with lot acceptance of the gear substrate materials. By demonstrating success on this battery of tests, it could be demonstrated that the application of the coating does not affect key material properties deemed critical by designers.

The process of applying this coating system is done at relatively low temperatures, usually below 400°F. This allows the coating process to be the final production step for any treated gear, and the temperature exposure does not affect the heat treatment called for by the gear designer.

Test Methods and Results

Basic Tribological Testing

ASTM G133 (Ref. 10) is used as a coating evaluation test during development work. This test uses a ball-on-disc method, with a load imposed on the ball. The disc reciprocates, and the coefficient of friction is extracted from the force required to cycle the sliding element. This coating was tested with a coated disc (coupon), no lubrication, and a static load of 20 N applied to the interface. A tungsten carbide-coated ball of 6mm diameter was utilized for this test. This combination produced a contact stress of 320 ksi.

The apparatus cycled at 5 Hz (5.6 cm/s with a stroke length of 4 mm). This test was performed at 25°C, laboratory ambient temperature. The test was performed over a total interface travel of 1,000 m.

The results of the testing performed on the coated sample are compared to the results from testing using the bare substrate, with a surface finish equivalent to the value required for finished gears and the bare substrate with the recommended surface finish for applying the coating system. As discussed, the coefficient of dynamic friction is derived from the actuation forces necessary to produce motion. Additional metrics are gathered from the amount of wear present on both the coated test coupon and the test ball after the test.

Table 4 compares the performance of the substrate material and the coated substrate material. The coating tested had a total thickness of 3.5 µm. It is standard practice to recommend that surface finishes such as those achievable with isotropic superfinishing be specified in conjunction with applying thin film coatings to reduce friction and wear.

	Surface Finish (µin, R_a)	Coefficient of Sliding Friction (µk)	Normalized Test Ball Wear (mm³/N/m)	Normalized Coupon Wear (mm³/N/m)
1	32†	0.70	3.31×10^{-7}	2.15×10^{-6}
2	4	0.60	1.58×10^{-7}	9.40×10^{-7}
3	4 Coated with P51M	0.15	2.56×10^{-9}	8.92×10^{-8}

Table 4—ASTM G133 test data for AISI 8620 test coupons in coated and uncoated conditions.

† This is the surface finish specified on the gear manufacturing drawings.

Coating Characterization Testing

Testing used to characterize the adhesion and resilience of thin film coatings was also employed during this work. In addition to the thickness measurement test described in paragraph 1.6, the tests described here compare different coatings and monitor the repeatability of the coating process.

Figure 7 shows the result of a coating thickness test performed in accordance with ISO 26423, as discussed in reference to Figure 1. The coating thickness was optically measured to be 3.95 microns.

Figure 10 shows a section view, obtained with a scanning electron microscope, of the test crater illustrated in Figure 9.

The test used to evaluate coating adhesion, ASTM C1624 (Ref. 11), uses a stylus with a constantly increasing load to quantitatively characterize the adhesion performance of a coating. The coating is tested with a Rockwell "C" style indenter, with the test terminating when the normal force reaches 100 N. Three critical loads are identified in the standard, representing different levels and types of coating failure. These loads are captured with the help of a machine vision system, identifying the coating failure mode. The first critical load (LC1) is the load where the coating begins to exhibit chevron cracking, indicative of cohesive coating failure or failure of the coating to adhere to itself. LC2 is said to occur when the coating exhibits chipping

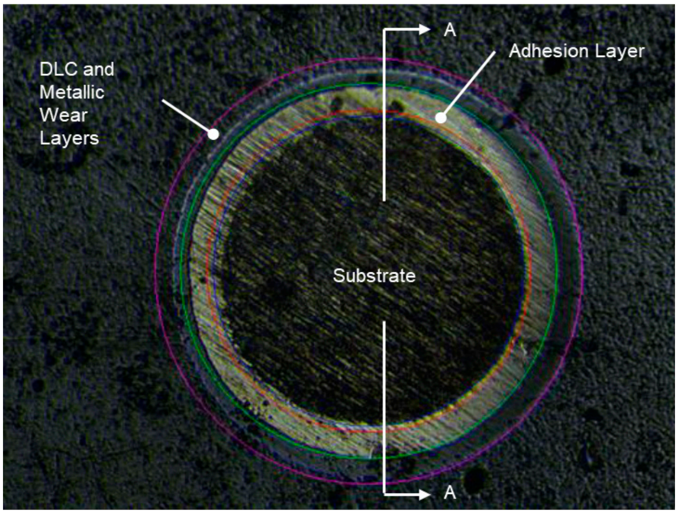

Figure 9—ISO 26423 Thickness Test on the P51M coating system.

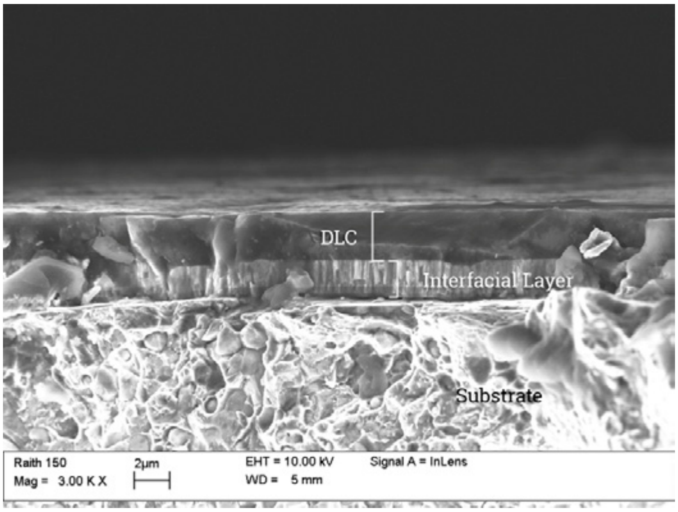

Figure 10—ISO 26423 Thickness Test on the coating system. This image is oriented as Section A-A of Figure 7.

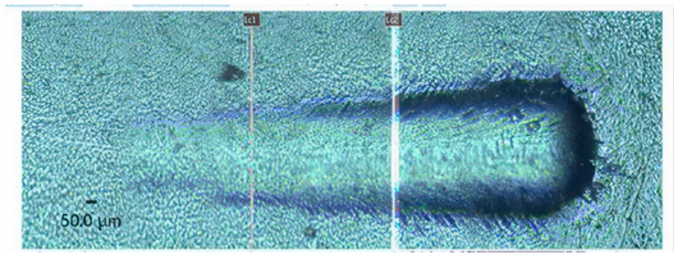

Figure 11—Image of ASTM C1624 Scratch Test results on P51M Coating. For this test, LC1 was detected at 33.3 N, LC2 was detected at 63.27 N, and no occurrence of LC3 was detected.

failure, indicative of an adhesive failure of the coating, or where the coating begins to spall away from the substrate at the edges of the damage zone. LC3 is the final metric, where the coating freely spalls away from the substrate. An image of the test impression is shown in Figure 11.

Mechanical Property Testing

Four different mechanical property tests were conducted on standard uncoated and coated specimens. The material used for testing was AISI 8620, which was machined and case-hardened to match the requirements shown on the gear drawings (HRC 60 and 0.010–0.020-in. case depth). An independent testing laboratory performed the mechanical property tests. The fluid contamination and thermal shock tests were performed in the laboratory facilities of the authors at UPT.

The following properties of the coated material were tested, using the test methods indicated in Table 5.

Mechanical Property	Test Method	Summary Result for Coated Parts
Tensile Strength	ASTM E8	7% average increase in tensile strength, 13% average increase in yield strength
Fatigue Strength	ASTM D790	8% average increase in number of cycles to failure
Shear Strength	ASTM B769	0.6% average increase in fracture strength
Compression Strength	ASTM E9	0.1% average increase in yield strength
Fluid Contamination	MIL-STD- 810G 504.2	No degradation
Thermal Shock	MIL-STD- 810G 504.2	No degradation

Table 5—Summary of mechanical property tests for coated test articles.

Please consult Ref. 12 for more details about test results.

Corrosion Resistance

Coated coupons, manufactured from AISI 8620 steel and carburized to match the gear drawings' specifications, were tested per MIL-STD-810G 509.6. This exposure to salt fog was accomplished in the author's laboratory. Figure 12 shows the coupons prepared for testing with edge sealant applied. All test articles have the coating under analysis on the exposed test surface. Test coupons have 1 in. dia. with a thickness of 0.25 in.

Figure 13 shows the coupon test articles after 24 hours of exposure.

After the initial 24-hour exposure was complete, the test articles were returned to the chamber for an additional 24 hours (48-hour total exposure). The results of that test are shown in Figure 14.

Normal testing is terminated after 48 hours of exposure in the procedure defined in MIL-STD-810G 509.6. The coupons that showed corrosion were analyzed under magnification. The corrosion present was attributed to holidays/pinholes (Ref. 13) in the coating, which can occur when the surface preparation for the material is inappropriate, when the coating application process is not fully developed, or when the

Figure 12—Test coupons, showing the sample numbers.

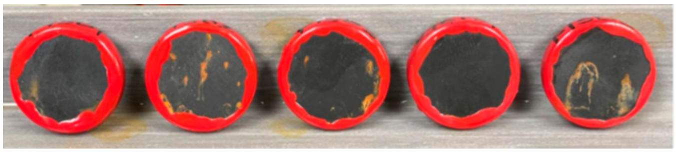

Figure 13—Test coupons from Figure 1 after 24 hours of salt fog exposure.

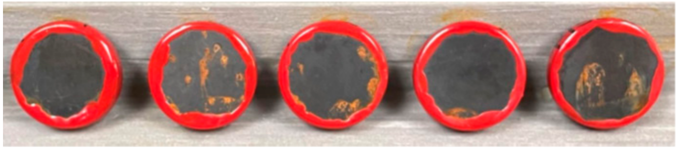

Figure 14—Test coupons from Figure 1 after 48 hours of salt fog exposure.

Figure 15—Test coupon F2703 after 1,341 hours of salt fog exposure.

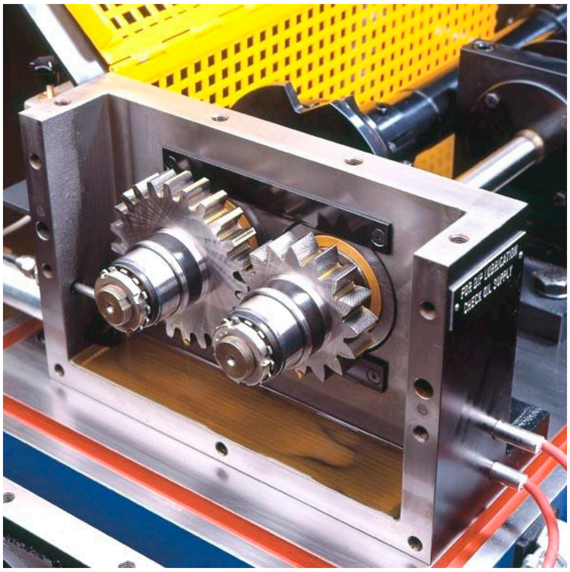

Figure 16—Open test cell in a standard FZG-type test machine, shown with a standard set of test articles with equal flank widths. The gear wheel has 24 teeth, and the pinion has 16 teeth (Ref. 15).

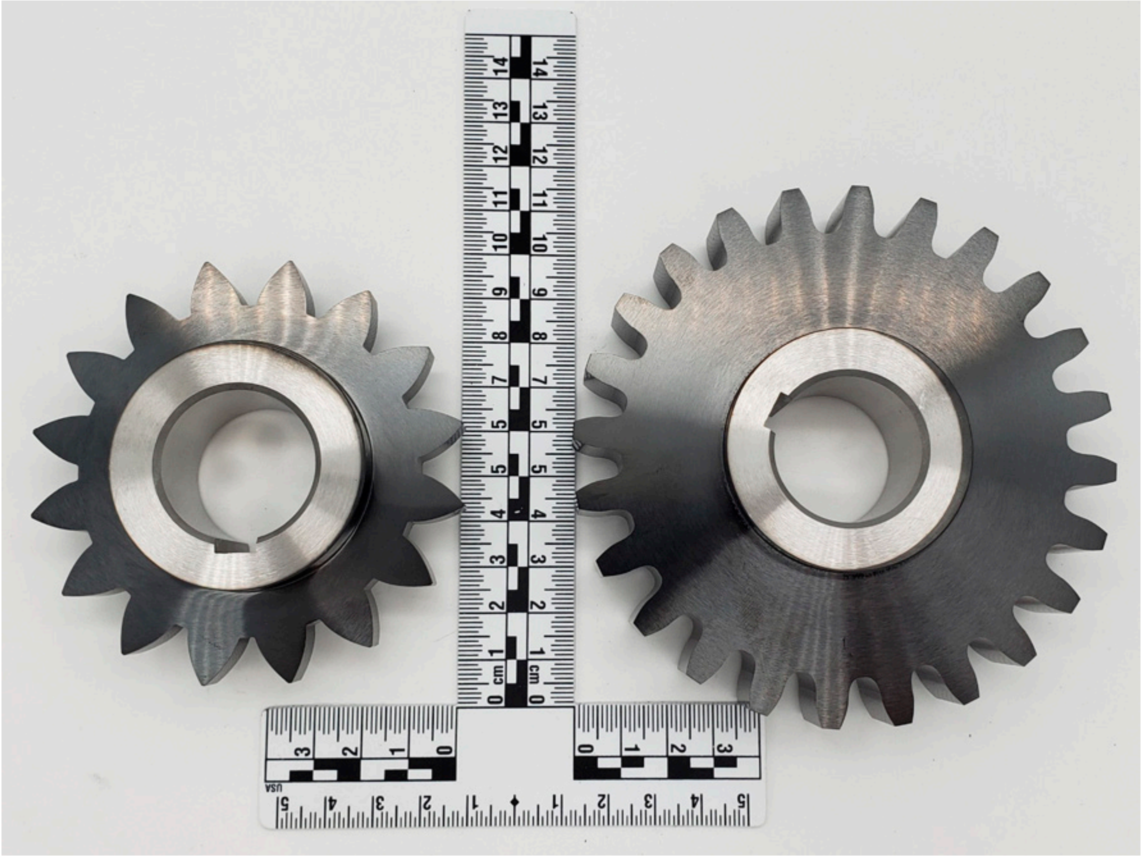

Figure 17—FZG test gears with P51M coating applied.

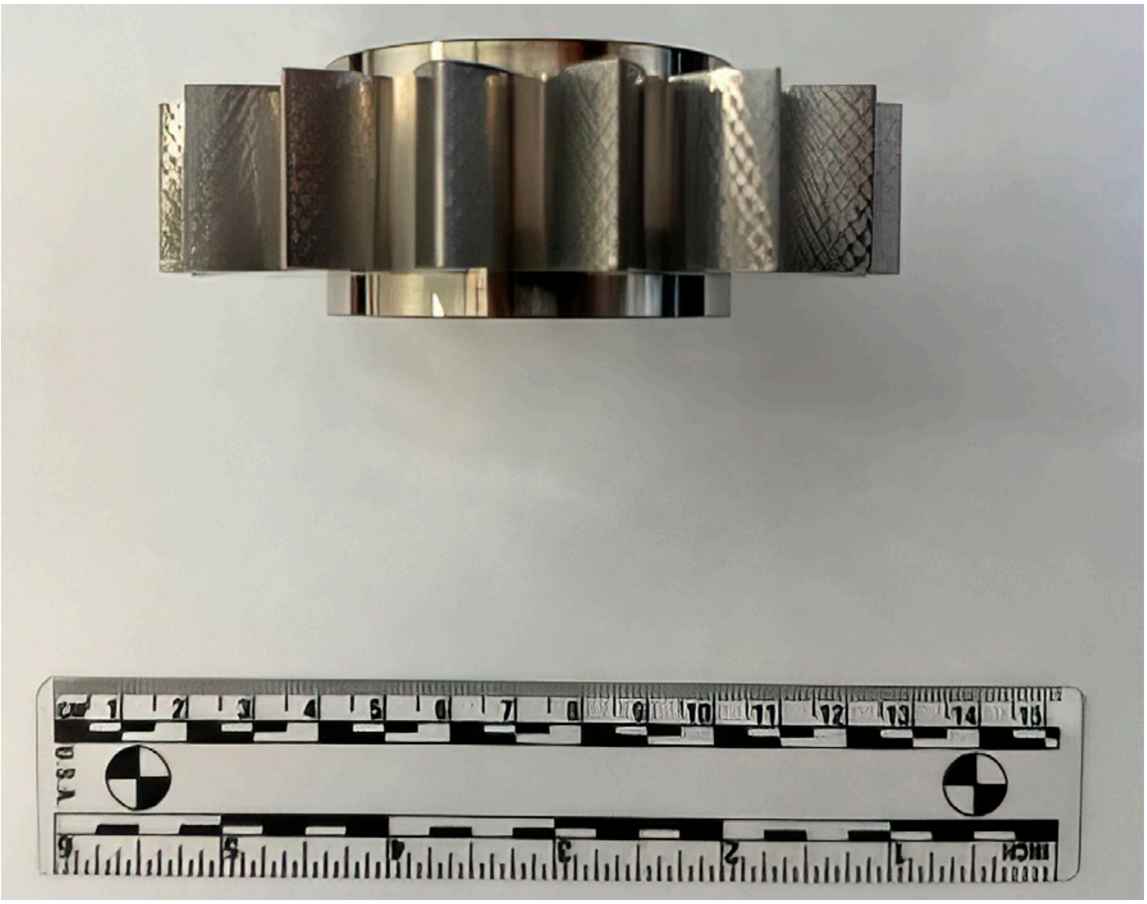

Figure 18—FZG test gear view of flanks showing the checked pattern used to highlight the appearance of surface scratches.

adhesion layer and associated surface modification design are not fully tailored to the chemistry of the substrate. The coupons that did not show signs of corrosion were returned to the salt fog chamber for long-term exposure.

Subsequent development of the adhesion layer and surface modification used with this coating recipe has yielded significant, consistent corrosion resistance performance for the coating system. Figure 15 shows a coupon manufactured from AISI 4140 steel. This coupon was removed from long-term testing to clear the chamber for new work. Based on the latest test results, the coating is rated for 1,000+ hours of salt fog exposure.

Shifted Profile Gear Scuffing Test

To translate the performance exhibited by the coating system under evaluation to a more application-specific test environment, methods used to evaluate liquid lubricants were explored. Shifted profile scuffing testing is commonly used to rate and compare liquid lubricants used in gear applications. The standard test, defined by ASTM D5182–Evaluating the Scuffing Load Capacity of Oils (FZG Visual Method) (Ref. 14), uses specially designed test gears manufactured from 20MnCr5 alloy (UNS G51200) steel. These gears have a shifted profile to increase the amount of slip at the mesh interface. The gears run in a four-square, dual-shaft arrangement, with ever-increasing torque loading applied through an adjustable clutch in progressive test stages. The test operator evaluates the scuffing wear on tooth surfaces and stops the test when there is a total scuffing area on the gear equivalent to a single flank width. Gears are also weighed before testing so that a material loss figure can be provided at the end of the test. Figure 16 shows a commercially available test machine with standard test gears mounted.

This setup uses the pinion as the drive input for the system. Previous experience and analysis of the results of tribological testing indicated that a more severe test was appropriate if coating failure was to be observed. A more severe version of this test is defined in ISO 14635-2: FZG test procedures Part 2: FZG step load test A10/16, 6R/120 for relative scuffing load-carrying capacity of high EP oils (Ref. 16). In this test, the gear wheel drives the system in reverse. Additionally, the pinion has a flank width of 10 mm (half of the gear wheel flank dimension), increasing the contact stress between the test articles. The independent test lab performing this work suggested that Mobil DTE Light Oil of ISO grade 32 (Ref. 17) be used as a test lubricant, as it would offer minimal protection to the gear surfaces themselves, minimizing any occlusion of results attributable to the coating. This is the test that was performed to evaluate the scuffing performance of the coating.

While the test gears were manufactured from 20MnCr5 alloy (UNS G51200) steel, the coating's adhesion performance is transferable to any ferrous substrate. The adhesion layer of the nanocomposite coating is not as sensitive to metallic substrate chemistry as it is to surface cleanliness. Additionally, the coating's adhesion performance improves as surface hardness rises due to the decrease in substrate deformation.

Figure 17 shows a set of test gears after application of the coating. Figure 18 shows a close-up of the test surfaces of an uncoated gear, with the checked pattern visible. This is a visual aid for the test operator when assessing failure. Due to the small coating thickness, this pattern was still visible after coating application.

Test results were reported in stages, given in Table 6. The lubricant bath temperature is also recorded to give information about the amount of heat generated at the mesh interface.

Test Stage	Operator Description	Calculated Contact Stress (MPa)	Calculated Contact Stress (ksi)	Oil Bath Temperature (°C)
1	No scratches on any teeth	206	30	40
2	No scratches on any teeth	417	60	40
3	No scratches on any teeth	670	97	50
4	No scratches on any teeth	878	127	120
5	No scratches on any teeth	1,093	159	125
6	No scratches on any teeth	1,314	191	125
7	No scratches on any teeth	1,527	221	125
8	No scratches on any teeth	1,730	251	130
9	No scratches on any teeth	1,960	284	130
10	Two teeth with two scratches each	2,176	316	135
11	Scratches on six teeth	2397	348	145
12	Scratches on all teeth	2,615	379	151
13	Failed, Sum of heavy scuffing on all teeth > 1 flank width	2,833	411	172

Table 6—ISO 14635 - 2 FZG test procedures Part 2: FZG step load test A10/16, 6R/120 for relative scuffing load-carrying capacity of high EP oils results for P51M. 1.4 Liters of oil were used for this test.

The failure stress is far more than the maximum allowable stress for grade 3 steel gears given in Ref. 7, of 275 ksi.

The pinion and gear wheel were weighed before and after the test. Table 7 summarizes the material loss due to scuffing because of this test.

	Weight prior to testing (g)	Weight after testing (g)	Weight Loss (g)	Weight Loss (ppm)
Gear Wheel	1,258.6196	1,258.0063	0.6133	487
Pinion	708.1166	707.9748	0.1418	200

Table 7—ISO 14635 test weight change data.

Ball on Disc Scuffing Test

Additional testing was done with an alternate method. A ball-on-disc method was employed to better control the contact surfaces' relative velocity. This test allows the user to specify the amount of sliding present at the contact interface where both sliding and rolling occur. In involute gear teeth, the contact is perfect rolling at the pitch diameter, with varying amounts of sliding in the rolling direction and in contrast to the rolling direction during every tooth contact event. A commercially available ball-on-disc scuffing test cell is shown in Figure 19.

Figure 19—Commercially available ball on disc test cell (Ref. 18).

The use of this apparatus also allows control over the surface finishes of the two surfaces in contact to more closely match the interface expected on gears treated with the coating system. The test parameters were the entraining velocity (U_e), the sliding velocity (U_s), and the velocity vector (v). These are defined by:

$$U_e = (U_b + U_d)/2 \tag{7}$$

Where U_b is the velocity of the ball and U_d is the velocity of the disc, and

$$U_s = U_b - U_d \tag{8}$$

The velocity vector is the resultant vector sum of the ball and disc velocities:

$$\vec{v} = \overrightarrow{U_b} + \overrightarrow{U_d} \tag{9}$$

Figure 20 provides a general schematic of the various velocities. T_b and T_d refer to the temperatures of the ball and disc test articles, which are also shown in the data plots presented.

The velocities used in testing were chosen as representative of the general gear geometry under study in this work. The test progresses much as does the shifted profile test. Increasing loads normal to the test surface are applied to the test articles, with the occurrence of scuffing events used to terminate a test. To more closely simulate service conditions, MIL-PRF-7808 fluid was used as the lubricant for this testing. This test was accomplished by an independent testing laboratory.

This test device monitors the traction coefficient, defined as:

$$T_c = \frac{F_T}{F_N} \tag{10}$$

where F_T is the traction force, and F_N is the normal force. This coefficient spikes sharply when the test articles begin to scuff due to dramatically increased friction between the moving surfaces, and this signal is used to terminate testing.

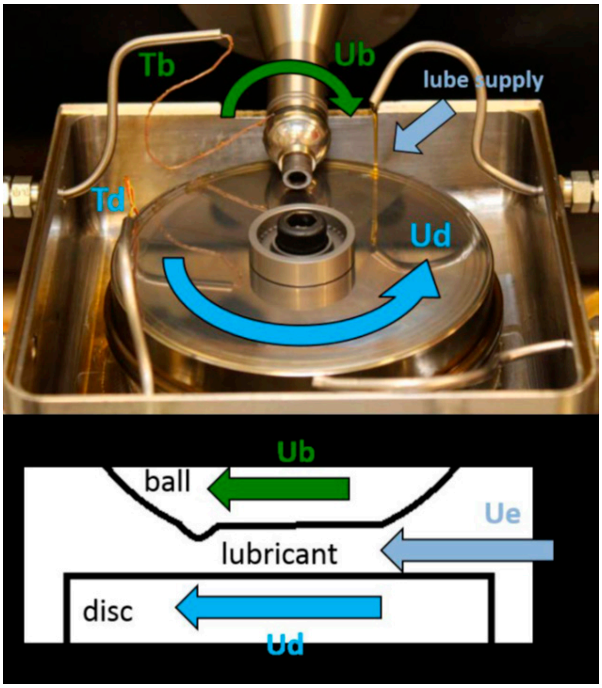

Figure 20—Schematic of forces in ball on disc testing (Ref. 19).

Table 8 provides test configurations and results for the various combinations of surface treatments evaluated. Figures 21–23 plot the test data.

Note that this test apparatus can monitor the temperature of both the ball and disc under test. The data for individual test cases are shown in Figures 19, 20 and 21.

	Ball Surface Finish (µin, Ra)	Disc Surface Finish (µin, Ra)	Entraining Velocity (m/s)	Sliding Velocity (m/s)	Velocity Vector Angle (degree)	Failure Stage	Contact Stress (ksi)
1	32	32	19.5	8.75	25.5	18	241
2	3	3	19.5	8.75	25.5	30	345
3	3 Coated with P51M	3 Coated with P51M	19.5	8.75	25.5	33	372

Table 8—Ball On disc test configurations and test results. All test articles were manufactured from AISI 8620 steel.

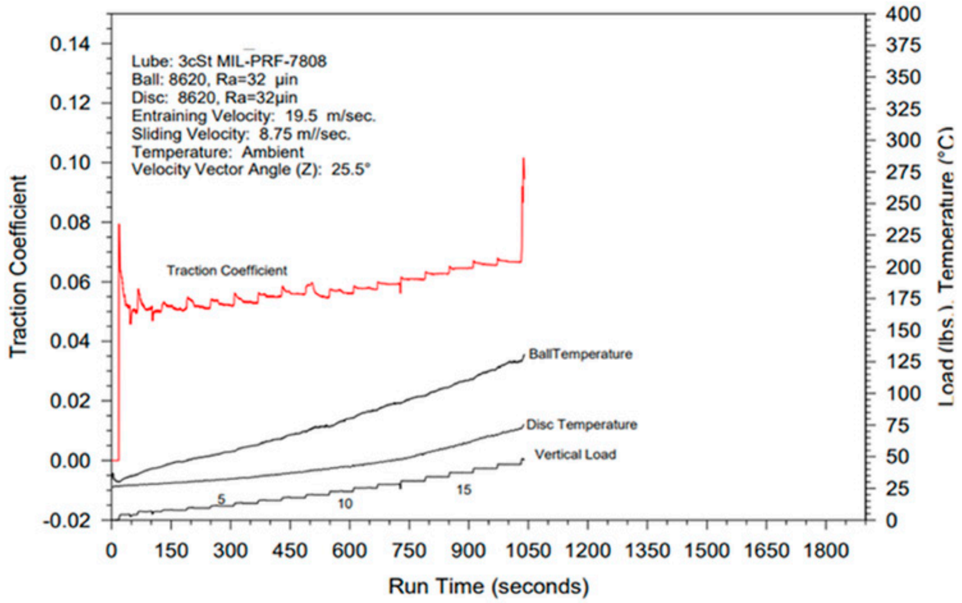

Figure 21—Data plot for the uncoated and unimproved surface finish ball on disc test articles with surface finishes representative of the gears under study.

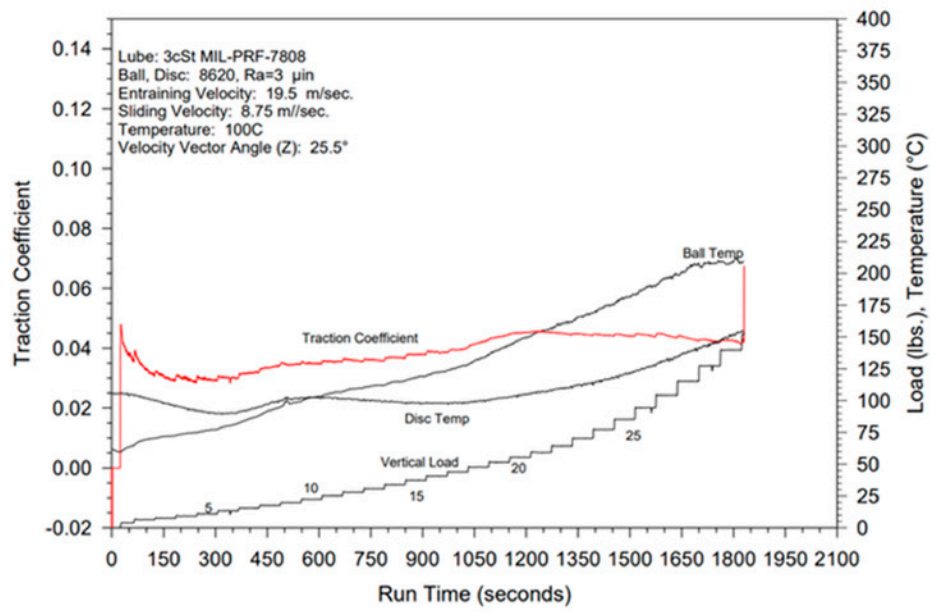

Figure 22—Data plot for the uncoated ball on disc test of test articles with improved surface finish. Note the scuffing event indicated by the traction coefficient data-trace at around t *= 1,800 s.*

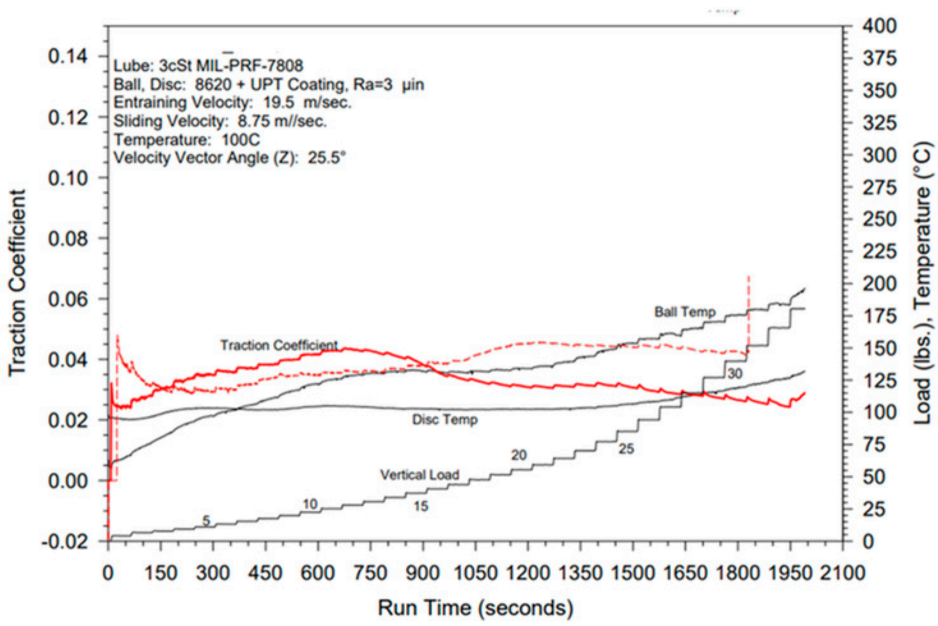

Figure 23—Data plot for the ball on disc test of P51M coated test articles. Note the lack of a spike in the traction coefficient. The red dotted trace is the traction coefficient of the uncoated ball on disc test, shown for reference.

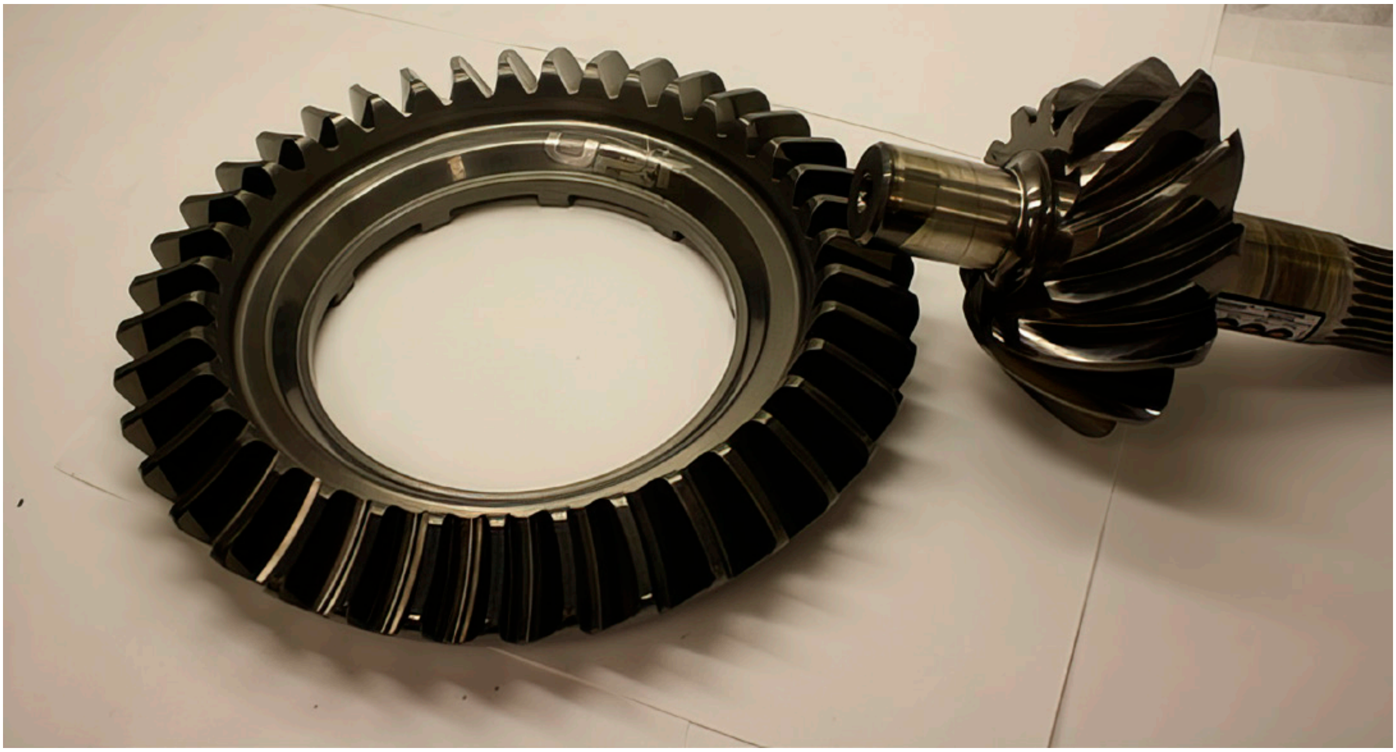

Figure 24—Ring gear and pinion from a competitive racing team, coated with the predecessor of the P51M coating system.

The differences illustrated in Figure 21 are the reduction in traction coefficient, reduction in ball and disc temperatures, and the higher load capacity when comparing the test articles with an improved surface finish and test articles with both an improved surface finish and the coating system applied. At stage 30, these are 0.04 compared to 0.02 for the traction coefficient, 225°C compared to 175°C for the ball, and 150 °C compared to 120°C for the disc. The load capacity increased from stage 30 to stage 33. The increase in contact stress is shown in Table 8.

Discussion and Future Work

The low coefficient of friction, improved wear resistance, and enhanced scuffing resistance exhibited by test articles treated with the nanocomposite coating under study indicate that further development is warranted. Improvement in wear resistance by multiple orders of magnitude, along with the drastic reduction in coefficient of friction, should yield significant benefits to many systems where gears are used. These laboratory results are compelling, but a demonstration in a testable application where the performance improvements of a system can be discerned will be necessary to achieve the level of confidence necessary to field this coating on a production basis.

This project was inspired by work done for a competitive racing team operating in an environment where any edge in performance is valuable and where significant engineering effort is expended to obtain such performance advantages. The ring and pinion for this project are shown in Figure 24. It should also be noted that a similar arrangement is being developed for UAV applications.

While the authors are constrained by a non-disclosure agreement with this racing team to release detailed data, the results obtained from dynamometer testing showed an average increase of 0.5 percent of operating torque available at the vehicle brake.

Conclusion

Nanocomposite coatings have been shown to be potentially beneficial to gear applications. The benefits of using these coatings are:

- Increased load capacity
- Decreased temperature of operation
- Corrosion resistance
- Retention of heat treatment state after coating
- Reduced friction between surfaces in mesh

Dr. Peter L. Schmidt, P.E., is the Lead Research Engineer at United Protective Technologies, LLC, based at the UNCC PORTAL office. He holds Bachelor's, Master's, and Doctoral degrees in Mechanical Engineering. With over 35 years of professional experience, Dr. Schmidt has worked in various sectors, including the Department of Defense, commercial manufacturing, consulting, and academia. He has held academic appointments at two universities, achieving the rank of full professor before joining his current firm. Additionally, he is a licensed professional engineer in two states.

Brady Blomquist holds a B.S. in Mechanical Engineering from BYU-Idaho and has worked as an aerospace engineer for the U.S. Air Force for five years. His work focuses on secondary power systems, including auxiliary power units (APUs) and gearboxes. He served as the government contact TPOC for this project.

References

1. C. Donnet and A. Erdimir, *Tribology of Diamond-like Carbon Films: Fundamentals and Applications,* New York: Springer, 2008.
2. S. Zhang and N. Ali, *Nanocomposite Thin Films and Coatings: Processing, Properties and Performance,* London: Imperial College Press, 2008.
3. United Protective Technologies, LLC, "United Protective Technologies," [Online]. Available: *https://www.upt-usa.com/* [Accessed 21 August 2024].
4. ISO, ISO 26423–Fine ceramics (advanced ceramics, advanced technical ceramics): Determination of coating thickness by the crater-grinding method, Geneva: International Organization for Standardization, 2009.
5. United States Government Small Business Administration, "America's Seed Fund - SBIR STTR," [Online]. Available: *https://www.sbir.gov/* [Accessed 16 May 2024].
6. United States Department of Defense, [Online]. Available: *https://media.defense.gov/2021/Sep/29/2002864141/-1/-1/0/180612-F-GX122-9174.JPG* [Accessed 24 April 2025].
7. AGMA, ANSI / AGMA 2001–Fundamental Rating Factors And Calculation Methods For Involute Spur And Helical Gear Teeth, Alexandria: American Gear Manufacturer's Association, 2004.
8. R. G. Budynas and J. K. Nisbett, *Shigley's Mechanical Engineering Design,* New York: McGraw Hill, 2020.
9. C. Maiorano, E. Pascale, F. Shekelberg, L. Bouillaut and P. Sannino, "MTBF (Metric That Betrays Folk)," in 29th European Safety and Reliability Conference, Hannover, 2019.
10. ATSM, ASTM G133–Standard Test Method For Linearly Reciprocating Ball-On-Flat Sliding Wear, West Conshohocken, PA: ASTM International, 2022.
11. ASTM, ASTM C1624–Standard Test Method for Adhesion Strength and Mechanical Failure Modes of Ceramic Coatings by Quantitative Single Point Scratch Testing, West Conshohocken, PA: ASTM International, 2005.
12. P. Schmidt, T. Simmons and M. Kaushal, "Nanocomposite Coatings for Gears," in American Gear Manufacturer's Association Fall Technical Meeting, Chicago, 2024.
13. Garrett, Johansen, Orlandić, Bashir and Raeissi, "Detecting Pinholes in Coatings with Hyperspectral Imaging," in 11th Workshop on Hyperspectral Imaging and Signal Processing: Evolution in Remote Sensing (WHISPERS), Amsterdam, 2021.
14. ASTM, ASTM D5182 Standard Test Method for Evaluating the Scuffing Load Capacity of Oils (FZG Visual Method), West Conshoshoken PA: American Society for Testing and Materials, 2019.
15. STRAMA MPS, "FZG GEAR TEST RIG," [Online]. Available: *https://www.strama-mps.de/en/solutions/test-rigs/fzg-gear-test-rig* [Accessed 10 May 2024].
16. ISO, ISO 14635 - FZG test procedures Part 2: FZG step load test A10/16, 6R/120 for relative scuffing load-carrying capacity of high EP oils, Geneva: International Organization for Standardization, 2023.
17. Exxon Mobil, "Exxon Mobil DTE Series Oil," [Online]. Available: *https://www.exxonmobil.com/marine/-/media/files/global/us/marine/products/pp-mobil-dte-named-series-v3lo.pdf?la=en%20&hash=9DB9F70E8A39CEE29119C4EB1C491743* [Accessed 10 May 2024].
18. PCS Instruments, "ETM Test Device," [Online]. Available: https://pcs-instruments.com/wp-content/uploads/2020/10/ETM-Brochure.pdf [Accessed 12 May 2024].
19. US Army Research Laboratory, "Ball-on-Disc Tribometer's Protocol Development: Loss of Lubrication Evaluation ARL TR 7588," Defense Technical Information Center (DTIC), Aberdeen Proving Ground, 2016.

Gleason Corporation

ACQUIRES FUBRI S.R.L.

Gleason Corporation today announced it has acquired 100 percent of the shares of Fubri s.r.l., located in Vigano, Italy. Fubri is a global market leader in the manufacture of gear cutting tools, specifically high-speed steel hobs, serving a variety of global end-markets for more than 85 years.

John J. Perrotti, Gleason chairman and chief executive officer, stated, "We have great respect for the Fubri team which has demonstrated a strong competency in delivering high quality tools with competitive prices and lead times. We are excited about this combination which will further build on our mission of Total Gear Solutions and allow us to further expand our ability to serve our global customer base."

Massimo Mandelli, chief executive officer of Fubri, commented, "Fubri has been a family company since its inception, but I can think of no better partner than Gleason to help guide our company into the future. We look forward to joining the Gleason team and serving the market in an even bigger and better way."

Fubri s.r.l., has been renamed as Gleason Cutting Tools s.r.l. and will retain its current management and employees in Vigano.

gleason.com

Star SU

ANNOUNCES SALES DIRECTOR FOR CUTTING TOOLS

Star SU, the marketing, sales, and service affiliate of Star Cutter Company, has announced the hiring of Scott Lukomski as sales director for cutting tools. Lukomski will report to Star SU president, Andreas Blind.

Scott Lukomski

In his role Lukomski will lead the Star SU Sales team across all cutting tool applications. His focus will be on serving customers in every possible way by providing leadership and coaching to account and area sales managers, directing management, partnering on key accounts, implementing sales strategies, and ultimately driving growth.

"We are very pleased to have Scott in this leadership role for Star Cutter, and already have him traveling to meet customers, partners, and team members in sales and throughout the company," said Blind. "Scott emphasizes customer satisfaction and fostering partnerships with all internal and external stakeholders. I am excited to have a partner with decades of relevant industry experience who will serve our customers with a confident and outgoing disposition.

Among that experience is an extensive background in sales, marketing, engineering and account management, with concentration in automotive and aerospace industries. Lukomski joins Star Cutter coming from his most recent position as sales and marketing director at Marposs Corporation. He has also held similar positions at Perception/ISRA Vision and Jenoptik Automotive.

I've long-admired Star Cutter not only for its collaborative, family-oriented culture, but also for its deep technical expertise and commitment to innovation," said Lukomski. "When the opportunity arose to join a team that's shaping the future of cutting tool technology, I knew it was the right fit. I'm excited to contribute to a legacy of excellence and help drive continued growth and customer success.

Lukomski studied mechanical engineering/technology at Lawrence Technological University and Schoolcraft College. He and his wife Tanya live in the Plymouth, MI area and have two grown children. When not working to solve productivity issues, he enjoys DIY projects and the great outdoors.

star-su.com

ECM USA

PARTNERS WITH SEW-EURODRIVE FOR FULLY AUTOMATED VACUUM FURNACE SYSTEM

SEW-Eurodrive's heat treatment team recently completed their fully automated in-house vacuum furnace system integrated with their patented Movi-Trans inductive energy power transfer system (pictured parallel with ECM's transfer system rails). SEW-Eurodrive partnered with ECM USA to commission a modular Nano vacuum furnace system completely integrated with advanced automation for their Lyman, SC facility in June 2023. This six chamber, 20 bar quench Nano vacuum furnace system provides maximum flexibility and integration utilizing the addition of 16 tempering positions, advanced solventbased washer (both oil and water-based contaminants), and robotic workload assembly/disassembly. Dunnage management is also being provided and fully automated within the robotics configuration. Specifically designed to run multiple materials (including carburized grades and tool steels) this system has the modular flexibility to adapt to future increased production demands for various load scenarios and processes.

ecm-usa.com

AGMA

ANNOUNCES AWARD WINNERS AT 2025 ANNUAL MEETING

The American Gear Manufacturers Association (AGMA) honored seven members at the 2025 AGMA/ABMA Annual Meeting in Austin, Texas last week. One member received the Lifetime Achievement Award. Also awarded were the Chair and Distinguished Service awards. Three outgoing AGMA Board members received Directors Awards.

Lifetime Achievement Award

Dr. Ulrich Kissling, president at KISSsoft was recognized with the Lifetime Achievement Award for his continuous dedication and contribution to the industry.

The Lifetime Achievement award is given by AGMA to rare individuals who have given years of service to AGMA and the global gear industry. Dr. Kissling's practical experience and theoretical know-how, complemented by a passion and dedication to the world of gearing has helped him create KISSsoft into one of the most widely used gear design software products globally.

"Dr. Kissling has spent his entire career focused on gear and bearing accuracy, actively participating on ISO technical working groups, providing test data and methodology, and for ultimately creating a software system used globally be leading power transmission companies in order to design world class power transmission solutions," noted Michael Cinquemani, chair of AGMA and CEO of Master PT. Cinquemani presented the award to Dr. Kissling at the banquet dinner. "Kisssoft continues to be one of the go-to resources for gear design, and the industry will leverage what Dr. Kissling created for decades to come."

Chair Award

Greg Estell, founder and managing partner, The Estell Group was honored with the 2025 Chair Award.

The award is presented by the American Gear Manufacturers Association to an individual who has contributed in a meaningful way to the promotion of the gear industry, acted above and beyond the call of duty to support AGMA.

Greg has served in leadership roles on both the AGMA Board and the Foundation Trustee Board. In these positions, he has always made himself available to his peers and AGMA staff members to help make industry connections, international connections, and more.

"Greg doesn't just serve on a board, he gives both his time and money to support the activities of whatever he is engaged in," added Cinquemani. "During his time at the AGMA Foundation, he provided unique opportunities for members to engage, and support the efforts of the Foundation, especially scholarships. We can't thank Greg enough for his efforts to support the PT sector."

Distinguished Service Awards

Prakash Kadam, managing director of Pragati Transmission and Fred Eberle of Strattec (retired) received the Distinguished Service Award for their dedication to the association and the industry.

Prakash Kadam has advanced the gear industry significantly through his hands-on involvement in all processes within his company. His vast knowledge, innovative thinking, and passion for quality have directly influenced the industry by setting higher standards for gear manufacturing. Prakash will accept his award later this year at MPT EXPO.

Fred Eberle has worked for decades in the advancement of plastic and powder metal gearing in the automotive actuator market by developing new applications using these types of gears that have created value for end users of these products.

In terms of the gearing industry, Fred has worked with AGMA on several committees over the years, including twice serving as chair of the Powder Metal Committee and also serving as chair of the Plastics Gearing Committee.

"Both Prakash and Fred distinguished themselves with their long-time support and commitment to the industry and the sector," added Cinquemani. "Volunteers come from all over the world, and both of these AGMA leaders are wonderful examples of giving back."

Board of Directors Awards

During the AGMA Member Business Session, the following leaders were given Board of Directors Awards:

- Joe Goral, director of sales and marketing, Bourn & Koch, Inc.,
- Nicole M. Wolter, president and CEO, HM Manufacturing, and
- Scott Yoders, vice president—sales, Liebherr Gear Technology, Inc.

Michael Cinquemani, Scott Yoders, Nicole M. Wolter, Joe Goral

Each served three-year terms on the AGMA Board and played important roles in developing new programs for AGMA, including advocacy and EV training. "We thank them for their commitment and service to the industry, and we look forward to Scott Yoder's continued leadership as he takes on a new industry volunteer leadership as the AGMA Foundation Chair beginning in May."

agma.org

JUNE 15–18

PowderMet2025

PowderMet2025 (Phoenix) is dedicated to metal powder and particulate materials-based processes including press and sinter, metal additive manufacturing, metal injection molding and more. The show provides an energetic forum to showcase PM, metal AM, and MIM equipment, powders, products, and services. MPM2025, colocated with PowderMet 2025, is a technical conference and exhibition dedicated to metal additive manufacturing. Attendees can dive deep into the latest advancements in the field through insightful technical presentations and explore exhibits showcasing additive manufacturing technologies. Sessions include topics on material development, standards, metal density, and more.

geartechnology.com/events/powdermet-2025

JUNE 24–27

Automatica 2025

Automatica 2025 (Munich) examines how robotics and smart automation is changing the future. Focus topics include digitalization and AI, sustainable production, and workforce development. Apart from concrete practical applications and product innovations, attendees can exchange ideas with key players and industry experts. Showcases include mobile robots, service robots, smart maintenance, AI technology, connected machines, testing, startups and more.

geartechnology.com/events/automatica-2025

JULY 9–10

Dritev 2025

The automotive congress Dritev (DRIvetrain Transmission Electrification Vehicles) offers the powertrain community an optimal platform for exchange. Every year, decision-makers, experts, and industry leaders from around the world meet in Baden-Baden, Germany. Here, vehicle manufacturers and suppliers exchange ideas and capture innovations, developments and challenges in drive technology. During the two-day congress, experts from OEMs, suppliers and universities present practical lectures on new trends as well as classical topics in drive technology.

geartechnology.com/events/dritev-2025

SEPTEMBER 10–12

11th International VDI Conference on Gears 2025

The 11th International VDI Conference on Gears 2025 will be held in Garching, Munich at the Gear Research Centre (FZG) of the Technical University of Munich. Supported by national and international associations, the conference brings together 500+ leading experts from the international gear and transmission industry. Visiting the conference gives attendees the opportunity to take part in this leading international forum and learn about the latest developments and research results in the powertrain industry and academia. The conference is a unique meeting point for propulsion system manufacturers and researchers of gear and transmission systems.

geartechnology.com/events/11th-international-vdi-conference-on-gears-2025

OCTOBER 21–23

Motion + Power Technology Expo 2025

Produced by AGMA, Motion + Power Technology Expo (Detroit) is a three-day show that connects professionals looking for motion power solutions with manufacturers, suppliers, and buyers. Attendees will find new power transmission parts, materials, and manufacturing processes. Buy, sell, and get business done with organizations in aerospace, automotive, agricultural, energy, construction and more. Forge partnerships at one of the largest gatherings of CEOs, owners, engineers, sales managers, and other professionals in the electric, fluid, mechanical and gear industries. End-users can shop the latest technology, gear products, and services from leading manufacturers. No matter your industry, you will find new ideas and solutions that can benefit your plant and company.

geartechnology.com/events/motion-power-technology-expo-2025

AD INDEX

gear TECHNOLOGY®

FREE SUBSCRIPTION

24GTALL

☐ Renew my subscription ☐ NEW subscriber

☐ **YES** I want to receive/continue to receive ***Gear Technology*** ☐ **NO**

Name ______________________

Job Title ______________________

Company Name ______________________

Company Address ______________________

City ______________________

State ______________________

Zip Code ______________________

Signature: ______________________ *(required)*

Date: ______________

Please send

☐ PRINT Version

☐ DIGITAL Version (E-mail required)

E-MAIL: ______________________

☐ BOTH Print and Digital

*You can OPT OUT at any time.

How are you involved with Gears?

(Check all that apply)

☐ My company **MAKES** gears

☐ My company **BUYS** gears

☐ I **DESIGN** gears

☐ I am a **SUPPLIER** to the gear industry

☐ Other (please describe)

____

What is your company's principal product or service?

____

Your mailing label on the cover looks like this:

X/Y - means you have recieved a complimentary copy. Please complete this form to continue receiving your FREE copy of *Gear Technology*.

Q14 (shown above) - means you have 14 issues remaining in your subscription (a NEW subscription has 16 issues).

Q1 - means you have 1 remaining issue before your *Gear Technology* subscription expires. Please complete this form to renew.

MAIL to: 1001 N. Fairfax St, Suite 500, Alexandria, VA 22314 USA | SCAN to: *subscribe@geartechnology.com* | FAX to: 1.847.437.6618

Simulation, Signals and Soundwaves

Matthew Jaster, Senior Editor

There was a moment early at Automate 2025 when the back of the exhibition hall sounded almost "techno-symphonic." The low-fi hums of robots, linear guides and AMRs treated the attendees to a 9:00 am orchestra of beeps, bleeps, whirs and clicks—a steady, impressive beat if you listened carefully. This musical odyssey suggested robotics and automation can be so much more than enhanced tools for warehouses, assembly lines and laboratories—and after a little research this was easily confirmed.

Mad Scientists

"Finis Musicae (*finismusicae.com*) brings to life a robotic orchestra controlled by human biometrics." According to the website Finis Musicae expands the borders of robotics, musical artistry and ultimately humanity. Fusing converging technologies, the project aims to usher in the automata age, anthropo-centralized.

Previously the secret research project of Fredrik Gran, robotics director, Charlotte Kemp Muhl, director and Sage Morei, creative and tech director, Finis Musicae offers transhuman anatomy extenders, "designed to improve the lives of people with disabilities, enable remote collaboration between artists with telekinesis and physical robotic avatars, and ultimately perform Beethoven in space."

The name Finis Musicae refers to the debut of the first electronic instrument. The talented group utilizes servomotors, computers and 3D-printed end effectors to prove AI and automation will not replace human creativity but help in its evolution. The project expands human potential through mechanical and digital transhumanism, exploring experimental compositions in new genres, and provides what the musical community is calling "an anti-dystopic vision of tech."

The Robotic Cello

According to the music magazine *The Strad* (*thestrad.com*), a cello played by a robot performed alongside a symphony orchestra in Malmö, Sweden last October. The performance premiered the new work Veer (bot) for orchestra and robot cello, written by Swedish composer Jacob Mühlrad, blending classical music with modern influences, pushing the boundaries of music with the aid of technology.

The robot cello combines industrial robotic arms with 3D-printed parts, designed by researcher and composer Gran of Finis Musicae. The instrument aims to challenge listeners' traditional notions of musical performance. "The robot is itself an instrument controlled by my notes. In a way, the composition and the instrument are brought together on an even deeper level," said Mühlrad to *The Strad*.

Maestros and the Machines

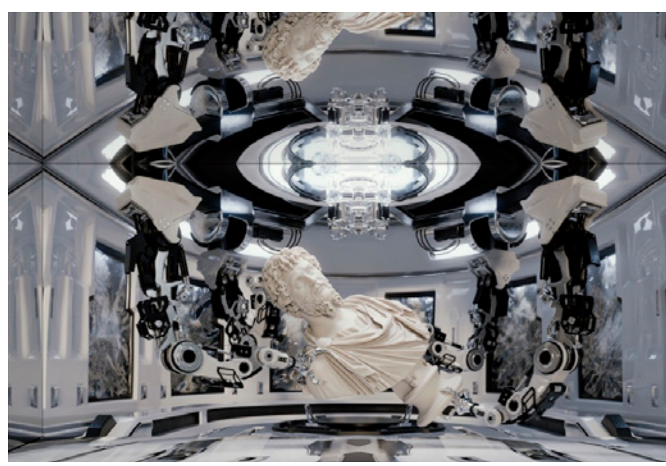

Mercer Labs, Museum of Art and Technology (New York, NY) recently unveiled "Maestros and the Machines," an exhibition inviting visitors to imagine what the great maestros of the past—from Mozart and Da Vinci to Hokusai and more—would have created if they had access to modern technology. "Maestros and the Machines" is a living, breathing dialogue between past and future, reimagining what art can be in a world where technology is a tool to the creative process. The exhibition was conceived and directed by artist Roy Nachum.

Nachum is an experimental artist known for his comprehensive artistic practice that spans across various mediums, including painting, sculpture, architecture, installation and technology. These works utilize art historical elements, conceptualism, and interactivity to explore complex psych-visual factors (*mercerlabs.com*).

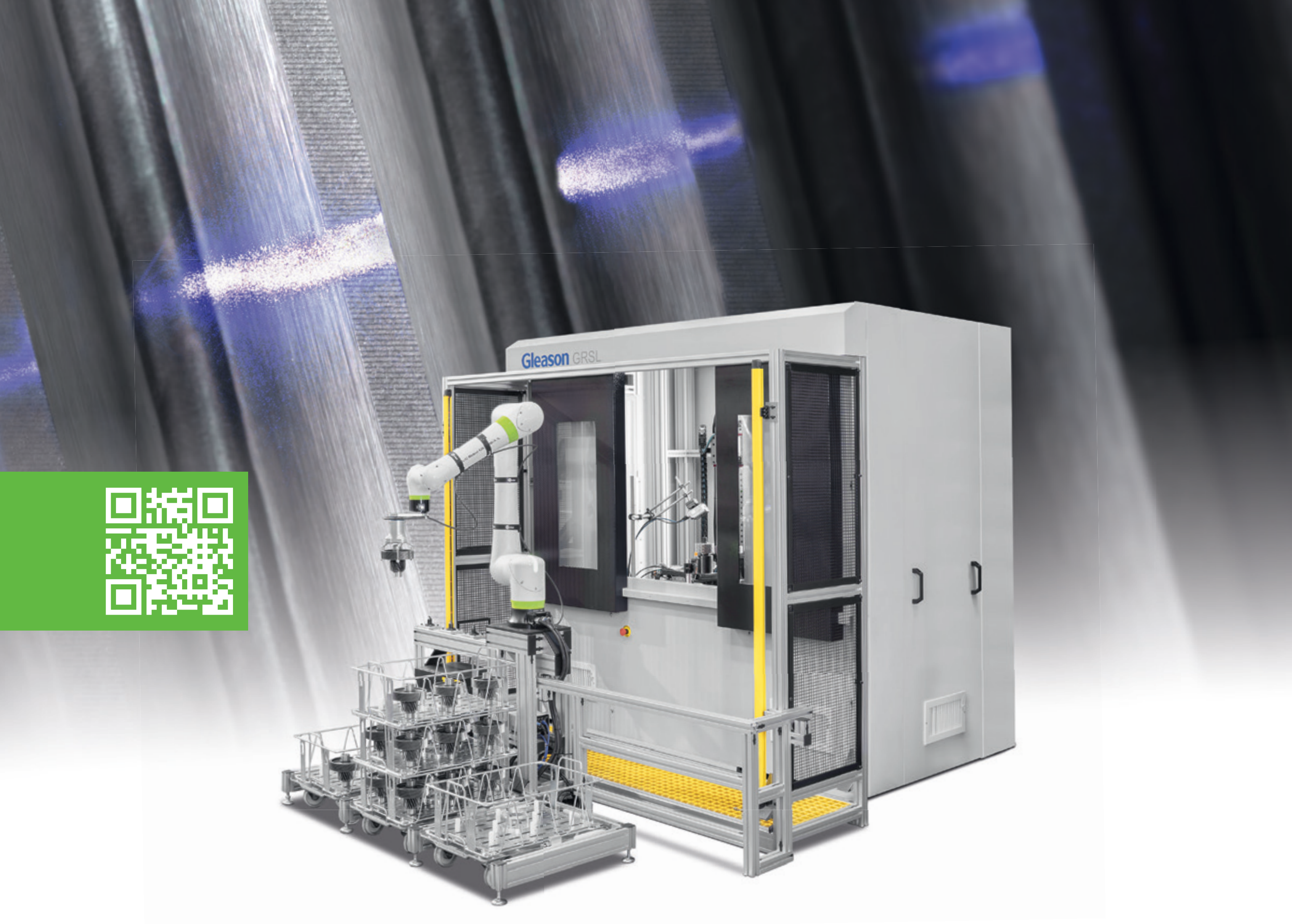
Gleason GRSL